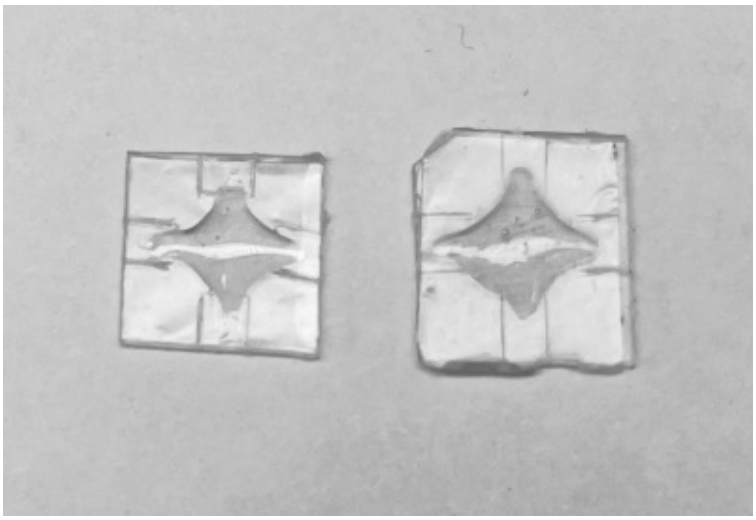

Effect of adhesives on characteristics of CVD graphene

An experimental study of graphene properties after its transfer to a substrate with the help of different adhesives

Master's thesis in Materials Engineering

CHARLOTTA ELVIND

DEPARTMENT OF MICROTECHNOLOGY AND NANOSCIENCE

CHALMERS UNIVERSITY OF TECHNOLOGY
Gothenburg, Sweden 2024
www.chalmers.se

MASTER'S THESIS 2024

Effect of adhesives on characteristics of CVD graphene

An experimental study of graphene properties after its transfer to a substrate with the help of different adhesives

CHARLOTTA ELVIND

CHALMERS
UNIVERSITY OF TECHNOLOGY

Department of Microtechnology and Nanoscience
Chalmers University of Technology
Gothenburg, Sweden 2024

Effect of adhesives on characteristics of CVD graphene
An experimental study of graphene properties after its transfer to a substrate with the help of different adhesives
CHARLOTTA ELVIND

Supervisor: Munis Khan, Microtechnology and Nanoscience,
Chalmers University of Technology
Examiner: Avgust Yurgens, Microtechnology and Nanoscience,
Chalmers University of Technology

Master's thesis 2024
Department of Microtechnology and Nanoscience
Chalmers University of Technology
SE-412 96 Gothenburg
Sweden
Telephone +46 31 772 1000

Cover: Graphene transferred to two substrates with top glues applied.

Typeset in LaTeX
Printed by Chalmers Reproservice
Gothenburg, Sweden 2024

Effect of adhesives on characteristics of CVD graphene
An experimental study of graphene properties after its transfer to a substrate with the help of different adhesives
CHARLOTTA ELVIND
Department of Microtechnology and Nanoscience
Chalmers University of Technology

Abstract

Characteristics of graphene when transferred using various adhesives have been investigated. The primary objective was to identify an adhesive capable of withstanding elevated temperatures common in photolithography (100-150°C) without compromising graphene properties. The project consisted of three parts. First, the graphene growth by chemical vapor deposition (CVD) was optimized by adjusting gas flow rates during the process and input parameters such as time and temperature. The quality of the graphene was examined at different regions of the copper foil used as a catalyst in CVD. Second, the impact of different adhesives on graphene doping and charge-carrier mobility was explored. Finally, the role of multilayer patches in graphene's interaction with adhesives was discovered by applying different adhesives to both sides of the graphene.

Keywords: CVD, Transfer, Adhesive, SEM

Acknowledgements

I want to thank all those who have supported me throughout this project. Avgust Yurgens and Munis Khan, thank you for your guidance, feedback, and continuous encouragement. Their expertise and dedication were instrumental in shaping the direction and outcome of this work. I also wish to thank the Department of Microtechnology and Nanoscience for providing the necessary resources and facilities to conduct my thesis and MyFab for support and access to the nanofabrication laboratory at Chalmers. I would also like to thank Emma Sandström at GA Lindberg for providing me with adhesives to work with during this work.

Finally, I would like to acknowledge my gratitude towards my family, who have supported my work, and all my friends, who have been there for me throughout this journey.

Charlotta Elvind, Gothenburg, August 2024

List of Acronyms

Below is the list of acronyms that have been used throughout this thesis listed in alphabetical order:

2D	Two Dimensions
3D	Three Dimensions
CVD	Chemical Vapor Deposition
DGEBF	Bisphenol F Diglycidyl Ether
DI	Deionized
EVA	Ethylene-Vinyl Acetate
h-BN	Hexagonal Boron Nitride
LEED	Low-Energy Electron Diffraction
PEEK	PolyEtherEtherKetone
PET	PolyEthylene Terephthalate
PMMA	PolyMethylMethAcrylate
SEM	Scanning Electron Microscopy
VDP	Van der Pauw

Nomenclature

Below is the nomenclature of parameters used throughout this thesis.

B_z	Magnetic field, z-direction
μ	Carrier mobility
n	Carrier concentration
E_F	Fermi energy
E_H	Hall field
F	Force
I	Current
K	A carbon atoms within graphene unit cell
K'	A carbon atoms within graphene unit cell
L	Length
q	Electron charge
R_s	Sheet resistance
t	Thickness
t_{gr}	Growth time
T_a	Annealing temperature
T_m	Melting temperature
T_{degr}	Degradation temperature
T_{gr}	Growth temperature
V_H	Hall voltage
V_x	Electric potential, x-direction
W	Width

Contents

List of Figures

List of Tables

1

Introduction

This thesis was executed at Chalmers Department of Microtechnology and Nanoscience in Gothenburg, Sweden. The sample fabrication was performed in Myfab Nanofabrication Laboratory. This chapter will briefly describe the background of this thesis and the aim, objectives, and limitations of this work.

1.1 Background

Graphene has been studied since the 1940s when Philip Wallace wrote a paper about the electronic structure of graphite [1]. The term "graphene" was coined in 1986. Polycyclic aromatic hydrocarbons are named with the suffix *-ene* to mark their simplest form. Since a single layer of carbon atoms was considered the simplest form of carbon, it was named *graphene* [2]. In 2004, graphene was isolated using mechanical cleavage, such as repeated application of Scotch tape [3], leading to the awarding of the Nobel Prize in Physics to Andre Geim and Kostya Novoselov in 2010.

Graphene, composed of carbon atoms bonded in a recurring honeycomb pattern, is a 2D material exhibiting promising characteristics suitable for various products. In sensor applications, the advantageous properties of graphene include high charge carrier mobility, the speed at which carriers move in response to an electric field, and low residual charge density. Currently, chemical vapor deposition (CVD) is a widely adopted method for graphene synthesis. During this process, hydrocarbon gas undergoes heating, leading to thermal decomposition (pyrolysis) and release of carbon atoms forming a graphene layer, typically on a copper foil substrate. Copper is a catalyst that accelerates pyrolysis. During growth in a CVD process, the optimal result would be a single layer. To achieve this, the input parameters for the CVD need to be optimized since the graphene tends to grow with patches, i.e., double layers, that are positioned closest to the copper foil in a CVD process. These patches affect the graphene's characteristics and are not desirable.

After a CVD process, the graphene must be transferred to a substrate. This is usually done in a wet transfer process. Here, the copper foil is spin-coated with PMMA, followed by removing the copper with an etchant. The PMMA is placed on a substrate, and PMMA is dissolved in acetone. This process is considered a type of double transfer since graphene is first transferred to PMMA, which is referred

to as the preliminary substrate in this thesis, and then to the final substrate. The downside of this type of transfer method is that the graphene can be contaminated during the process. Khan et al. direct-transferred graphene from copper foil to an office lamination foil composed of an Ethylene-Vinyl Acetate (EVA) adhesive layer on a PolyEthylene Terephthalate (PET) sheet [4]. Here, they placed the copper foil on such a lamination foil and laminated it in an office laminator, followed by etching the copper. The EVA's melting temperature depends on the content of Vinyl Acetate and can vary between 50-100°C [5]. EVA on the lamination foil melts at 70-75°C [4]. This study demonstrates enhanced graphene qualities following sample annealing at 60°C. The annealing temperature should be lower than the melting temperature $T_a < T_m$ to preserve the material's structure integrity. Khan et al. captured SEM images of their samples, revealing the presence of bi- and tri-layers and wrinkles. Despite this, the samples exhibited high charge carrier mobility (6000-8000 $cm^2/(V \cdot s)$) after the overnight annealing at 60°C.

Compared to the wet transfer, which is called a double transfer in this thesis, the direct transfer has fewer steps where graphene can be contaminated. Also, the patches that grow between the monolayer graphene and the copper foil during CVD (Figure 1.1(a)) are positioned on top of the monolayer graphene after a direct transfer (Figure 1.1(b)) but placed below the monolayer graphene after a double transfer (Figure 1.1(c)).

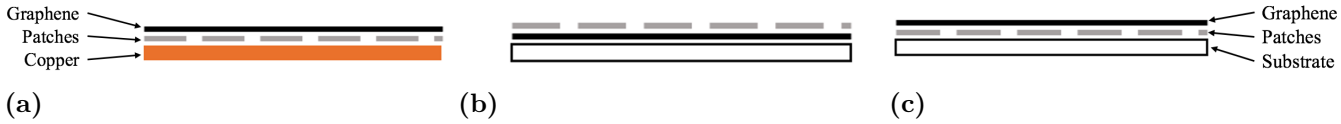

Figure 1.1: Patches as dashed lines and monolayer graphene as solid lines. Orientation of the patches **(a)** on the copper foil after a CVD process, **(b)** after a direct transfer, and **(c)** after a double transfer.

In conventional photolithography, a substrate is usually heated to evaporate any residual water from the surface (>100°C) for a few minutes. A layer of photoresist is applied with spin coating, followed by a soft baking process. A photo mask is applied to create patterns that selectively remove the photoresist. After this step, the wafer is typically subjected to wet etching or similar processes to create a pattern corresponding to the areas exposed. Removal of the remaining photoresist leaves behind the pattern delineated by the photo mask.[6]

For graphene to be applicable in photolithography, the adhesive used for transferring graphene must withstand >100°C, which is higher than the melting temperature of EVA.

1.2 Aim and objectives

This project aims to grow graphene and transfer it to a substrate with adhesives without worsening the quality of graphene compared with transfer on regular lamination foil (EVA/PET). The objectives for this thesis are:

- ☐ Optimize graphene growth in a CVD system and analyze the result.
- ☐ Direct transfer graphene with adhesives that can withstand >100°C.
- ☐ Double transfer graphene with adhesives that can withstand >100°C.
- ☐ Evaluate what influence the adhesives has on the graphene. How does it affect the transferred graphene?

1.3 Limitations

Graphene growth was conducted in a hot double-wall tubular system under sub-atmospheric pressure. Although this hot-wall system was not optimized for high-quality graphene production, it was used in this project for analysis purposes. A cold-rolled copper foil was used. The graphene was benchmarked against high-quality graphene that was commercially sourced and available; in this thesis, this graphene is called bought graphene. Characterization included measurement of sheet resistance (R_s), mobility (μ), and carrier concentration (n), collectively referred to as the quality metrics. Quality was only assessed with electrical measurements. Photolithography was not processed in this thesis. Patches, multilayers, and positional variations in graphene were not examined. Low energy electron diffraction was needed to examine if multilayers are positioned on top of monolayer graphene or between the monolayer and copper foil in a CVD process. This procedure was not included in this study. Instead, the literature study found that patches develop between the monolayer and copper foil in the CVD process. This was assumed to be true for all graphene grown on copper in this study. In this study, the wet transfer process was called a double transfer process, and PMMA was referred to as a preliminary substrate.

2

Theory

This chapter provides a short overview of the theoretical principles. It covers the key aspects of graphene theory, including graphene properties, doping, synthesis techniques, transfer processes, and imaging using SEM.

2.1 Properties & doping

Materials are generally divided into three groups: metals, semiconductors, and insulators. This can be illustrated with band diagrams, seen in Figure 2.1. Metals have overlapping bands, semiconductors have a small band gap, and insulators have a larger band gap. This band gap prevents electrons from reaching the conduction band. Therefore, metals are conductive materials since the bands overlap, i.e., electrons can move freely between the bands. An electric field can change the conductivity in a semiconductor and allow electrons to flow between the valence band and conduction band, despite the small band gap. A larger band gap requires a stronger electric field. Between the band gaps is the Fermi energy E_F. Fermi energy is the highest energy level occupied by electrons in a material at absolute zero temperature.

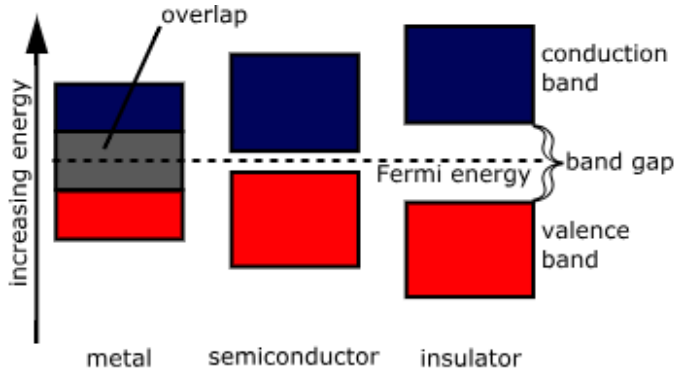

Figure 2.1: Band gap for metals, semiconductors and insulators. Image used via Wikimedia Commons. [7]

Carbon exhibits a range of allotropic forms, including graphene, graphite, diamond, and fullerenes. Each form possesses unique crystalline structures and properties. Graphene is a single-layer of carbon atoms arranged in a honeycomb lattice

and is also referred to as a monolayer. Graphene can also be two-, three- or a few layers. Graphene exceeding 10 layers is commonly termed multilayered graphene. The carbon atom has four valence electrons, but as seen in Figure 2.2, each carbon atom creates three covalent bonds and, therefore, only uses three of its four valence electrons to bond with neighboring atoms. This leaves one electron free for electronic conduction. In Figure 2.2, the unit cell of graphene is marked with dashed lines. It comprises two neighboring carbon atoms, labeled K and K' [8]. K points are illustrated in white; at each covalent bond, the carbon atom uses one electron, which is also illustrated in white. The same applies to K' points, which are marked in black.

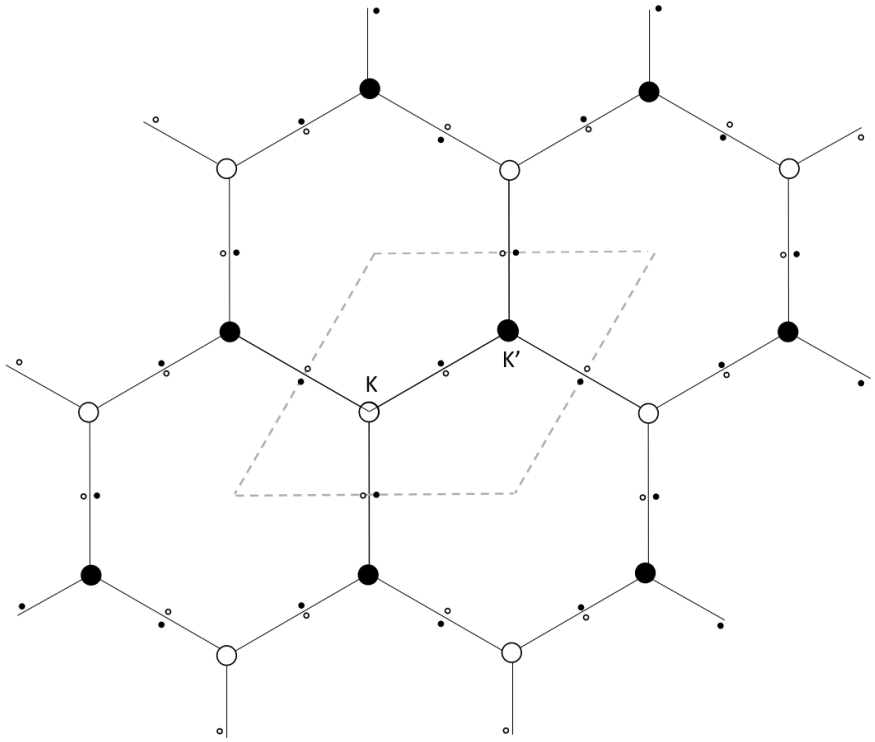

Figure 2.2: Honeycomb lattice of graphene with K and K' in the center of the unit cell. Each atom uses three valence electrons to create covalent bonds with the neighboring atoms. Shown as electron pairs between the atoms.

The band diagram for graphene can be illustrated in 3D. Linear approximation can be done as shown in the zoomed part of Figure 2.3. These are in each K and K' points. This linear approximation results in an effective zero mass of charge carriers, similar to photons. The Dirac equations describe these, hence termed Dirac points. The presence of Dirac points renders the band gap of graphene to be zero, classifying it as a semimetal. The Dirac point represents graphene's charge neutrality point, the intrinsic Fermi energy. As illustrated in the zoomed-in part of Figure 2.3, the valence band has electrons, and the conduction band has voids of electrons. These voids, i.e., the absence of electrons, are referred to as holes. Compared with Figure 2.1, the conduction- and valence band for single-layer graphene only connect at zero energy.

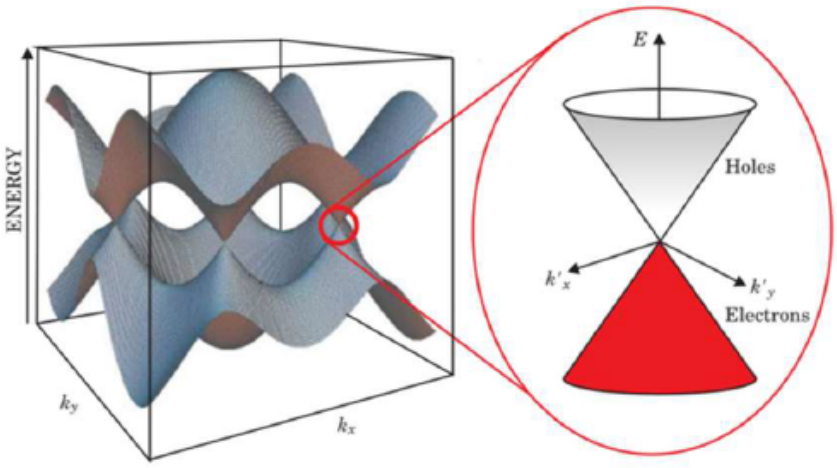

Figure 2.3: 3D band structure of graphene. Reproduced from *Electrons in atomically thin carbon sheets behave like massless particles* by Wilson, M., (2006), with the permission of the American Institute of Physics.[9]

Graphene can be used as a channel in a field effect application, as seen in Figure 2.4. This channel is connected with two metallic contacts at each end, and the graphene is placed on a Si/SiO_2 substrate that acts as the gate electrode. In this case, SiO_2 acts as a dielectric, and Si, which is usually heavily doped, acts as a gate. The gate electrode can be used to shift the E_F by applying a voltage. A positive voltage leads to electron domination, and E_F would move upwards, and the conduction band would start to fill up with electrons. A negative voltage moves E_F downwards instead. Consequently, the minimum conduction is achieved at the Dirac point; graphene has an ambipolar conduction behavior. [8]

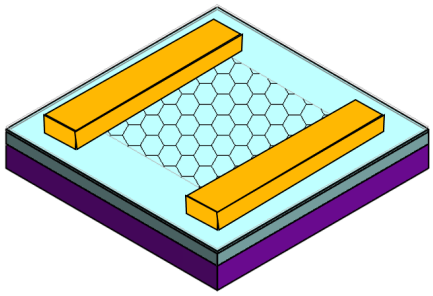

Figure 2.4: Basic geometry for graphene used as a channel in a field effect application. Graphene is contacted from both ends with metal contacts. Graphene is placed on a Si/SiO_2 substrate which is the gate electrode.

In semiconducting materials, doping involves the introduction of impurities into the crystal lattice. Considering carbon atoms belonging to the 4^{th} group of the periodic table, along with other elements such as silicon and germanium, doping can be achieved by incorporating elements from the 3^{rd} group of the periodic table. This results in p-type semiconductors as these elements possess only three valence electrons, increasing the possibility of an electron void, i.e. hole, in the crystal

structure. In Figure 2.2, all atoms have pairs of electrons between them, i.e., covalent bonds. If an atom that is introduced in the lattice does not have enough valence electrons to bond with neighboring atoms, a hole is created instead since an electron is missing. Alternatively, impurities from the 5^{th} group of the periodic table can be introduced, generating n-type semiconductors as these elements have five valence electrons, leaving extra electrons after forming covalent bonds. Doping with elements from the 3^{rd} group is referred to as *acceptors*, while those from the 5^{th} group are termed *donors* [10]. Doping graphene with atoms from the 5^{th} group introduces additional electrons, shifting E_F upwards, resulting in the partial filling of the upper cone with electrons in Figure 2.3. Conversely, adding atoms from the 3^{rd} group shifts E_F downwards, introducing additional holes and leaving some states unfilled in the bottom cone.

Graphene finds applications in various fields, such as photodetectors, photovoltaics, sensors, organic light-emitting diodes, organic thin-film transistors, supercapacitors, and catalytic processes. Achieving its desirable electronic structure and properties entails controlling the charge carrier concentration, typically accomplished via chemical or electrostatic doping. However, graphene's E_F is susceptible to change when graphene's surface is in contact with external matter, substrates, or environmental changes [11]. This is observed when graphene is transferred with adhesives since the adhesives are in contact with the graphene. The carrier concentration and sheet resistance can change during this process, shifting E_F up or down. While holes are dominant charge carriers in the sample, the carrier concentration is positive. Conversely, the carrier concentration is negative when electrons dominate. The graphene is therefore termed p-doped or n-doped, respectively.

Graphene's transport properties can be measured using van der Pauw's (VDP) method. This method applies to 2D materials and is used to measure a sample's resistivity and hall coefficient. Four probes are placed at the corners of a square sample, Figure 2.5(a), a current is applied along one edge, and voltage is measured across the opposite edge. This results in a resistance in both x- and y-direction. The mean value of these two resistances is multiplied by the VDP constant ($\pi/\ln 2$), resulting in the sheet resistance. With the same setup, the Hall effect may be observed. This effect is named after Edwin Herbert Hall, who observed the readings of a galvanometer when he passed a current through a sample placed within a magnetic field [12]. This phenomenon is commonly observed in semiconducting materials. It occurs due to the forces exerted by electric and magnetic fields on moving charges. One can determine whether the material is p-type or n-type through the Hall effect and measure the majority carrier concentration. A particle with the charge q experiences a force $F = qv \times B_z$ when subjected to a magnetic field, B_z, and moving with velocity, v. In a sample like the one depicted in Figure 2.5(b), current, I, flows perpendicular to the magnetic field, B_z. Electrons within the sample experience a force and accumulate on one side of the sample. This accumulation of charges induces an electric field, known as the Hall field, E_H, and results in a voltage across the sample, referred to as the Hall voltage, $V_H = E_H W$, where W is the width of the sample. The Hall voltage is positive for p-type semiconductors and negative for n-type semiconductors [10].

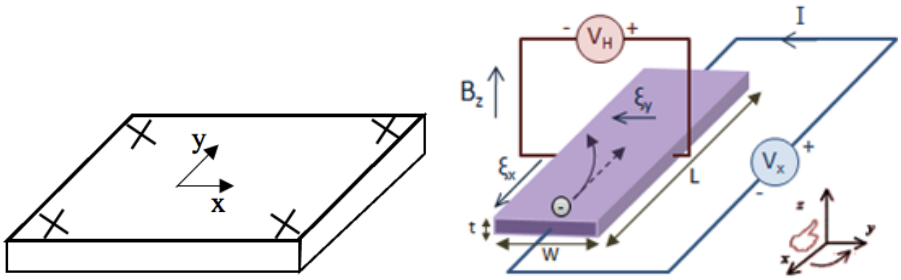

(a) **(b)**

Figure 2.5: **(a)** Square sample with four probes at each corner. Used for VDP's method to measure resistance in x- and y direction. **(b)** Hall effect measurement set up. Image used via Wikimedia Commons [13].

2.2 Synthesis

Graphene can be synthesized through various methods, categorized as top-down and bottom-up approaches. In the top-down approach, sheets of graphene are isolated from bulk graphite, typically achieved through chemical exfoliation and mechanical cleavage. Conversely, the bottom-up approach involves building graphene on a supportive substrate, with chemical vapor deposition (CVD) being the most commonly used method.

CVD is a process driven by thermodynamic and kinetic factors based on thermodynamics first and second laws. When carbon is involved in a CVD process, thermal decomposition (pyrolysis) of a hydrogen gas such as methane is necessary. Also hydrogen and argon is used in the process. Methane is typically pyrolyzed at temperatures exceeding 1100°C under pressures ranging from 100 Pa to 100 kPa. The simplified reaction formula is $CH_4 \longleftrightarrow C + 2H_2$. Three important deposition parameters for CVD with carbon atoms are pressure, C/H ratio, and temperature. Achieving graphene with uniformity, good coverage, and quality is often attained at low pressures. Pressure regulates the degree of diffusion, i.e., controlling how well and fast the gases spread and interact within the chamber. At low pressure, diffusion of the gas particles becomes more uniform, which makes surface kinetics the rate-controlling factor. Adding a non-reactive gas such as argon is necessary to prevent evaporation and re-condensation of copper. Argon is introduced into the CVD process as a carrier gas and remains chemically inert throughout the hot-wall CVD process [14]. The C/H ratio in the chamber plays a crucial role. Higher ratios tend to favor laminar and columnar deposits, i.e., carbon growing in parallel layers or columnar formation, not favoring single-layer growth of graphene. In summary, good uniformity is obtained at high temperatures, low pressures, and low C/H ratios. [15]

The most common metal foil used to grow graphene is cold-rolled. One can also use metal films. Films are produced by sputtering or thermal/electron evaporation and have more controlled film thicknesses. A single-crystal metal film is possible.

Metals that can be used are Cu, Ni, Pt, Ge, or Pd. The quality of graphene depends on the thickness of the metal, carbon solubility, and melting point [16]. Copper is the most commonly used foil for graphene CVD due to its price, availability, and low solubility of carbon in it [14]. When etching the copper in a transfer process, there are two main drawbacks; chemical residues degrade electronic properties and reduce mobility, and secondly, the copper is consumed, making the production method less efficient [17].

There are many studies on graphene growth by CVD. An article by Banszerus et al. describes a recipe for achieving high-mobility graphene in the CVD process [17]. After growth, graphene was sandwiched between hexagonal Boron Nitride (h-BN). Layers of h-BN was added to the graphene as outer layers to create a sandwich with graphene in the middle. The importance of the transfer method is also pointed to; this is crucial in getting high mobility in graphene. In an article by Yu et al., high mobility is reported for p-doped graphene [18]. Graphene is grown as individual grains, and its mobility is measured within a grain, i.e., intra-grain mobility. Yilmaz et al. examined the influence of the copper foil thickness and reported that a single layer was achieved on 150 µm foil [19]. They also pointed out the downsides of using thick foil, such as the need for more material and longer etching processes. In an article by Kalbac et al., two different isotopes of methane were used to examine the layers of graphene that grew [20]. $^{13}CH_4$ and $^{12}CH_4$ were induced for 3 min each. H_2 was used for 20 min to etch the double layers after growth. Quing et al. report 1-3 layers of graphene [21]. In a study by Wu et al., copper foil is prepared by cleaning it with acetone, ethanol, and DI water. During annealing, a mixture of Ar and H_2 (1500 sccm, 1.3% H_2) was induced in the chamber [22]. All the different studies on graphene growth analyzed in this thesis are summarized in Table 2.1.

During CVD growth, multilayers may form. These are visible as dark patches in an SEM image (technique discussed in section 2.4). The position of multi-layers during CVD growth has been discussed in previous research. The discussed topic is whether the patches are positioned on top of the monolayer or below i.e., between the monolayer and copper foil. Wu et al. write that multi-layer regions are on top

Table 2.1: CVD summary of graphene growth on copper in a hot walled chamber at sub-atmospheric pressure, found in earlier research. Note: "0" means no gas was used, "-" means no information of value

Ref	Annealing [min/°C]	[sccm] (H_2/Ar)	Growth [min/°C]	[sccm] (H_2/Ar/CH_4)	Transfer method	Etch	Resulting quality
[17]	20/1035	10/0	120/1035	45/0/1.3	hBN	Dry	50000 $cm^2/(V \cdot s)$
[18]	30/1050	10/300	10/1050	$10/300/8_{ppm}$	PMMA	$Fe(NO_3)_3$	10000 $cm^2/(V \cdot s)$
[19]	25/1000	50/100	5/1000	400/0/200	N/A	N/A	N/A
[20]	20/1000	50/0	6/1000	50/0/-	PMMA	NaOH	1 layer
[21]	30/1000	2/0	10/1000	2/-/35	PMMA	$FeCl_3$	1-3 layer
[22]	30/1050	1500	60/1050	$1500/10_{ppm}$	PMMA	$Fe(NO_3)_3$	1 layer

and smaller than the underlying layer [22]. They also suggest that a lower methane concentration is preferable for achieving single-layer graphene since the supersaturation of carbon atoms at the beginning of the growth causes multi-layers. The study by Kalbac et al. aimed to control the double-layer formation of graphene and reported that multi-layer graphene is at the center of the gains [20]. This suggests that the multi-layer graphene corresponds to the initial graphene seed. Patches form simultaneously as the single layer but grow at different speeds. Therefore, the double layer is named the slowly growing layer, and the single layer is named the dominating fast-growing layer. Also, claiming that the slowly growing layer is on top of the dominating fast-growing layer. This is because if the slowly growing layer is closest to copper foil, the carbon atom would need to enter between the copper foil and fast-growing graphene and travel a relatively long distance, lifting the faster-growing layer during growth, and all these events seemed unlikely. This theory was also supported by Robertson and Warner, who refer to these patches as few-layer terraces of graphene that are not in contact with the copper [23].

All these studies of graphene patches being on top of the main layer of graphene were published in 2011-2012. But Nie et al. published an article at the end of 2012 and proved that previous assumptions of the double layer growing on top of the single layer were wrong [24]. They proved that graphene patches grow as an inverted "wedding cake". However, the SEM images would look the same independent of whether the patches were on top or below the monolayer. So instead, they did low-energy electron diffraction (LEED), examining both the single- and two-layer regions, Figure 2.6. In these images, they see a honeycomb lattice of the same orientation and intensity at both the single-layer and double-layer parts of graphene. In the double-layer region, however, they also see another honeycomb lattice rotated by approximately 23° but with lower intensity. This proves that the single continuous layer is the top layer.

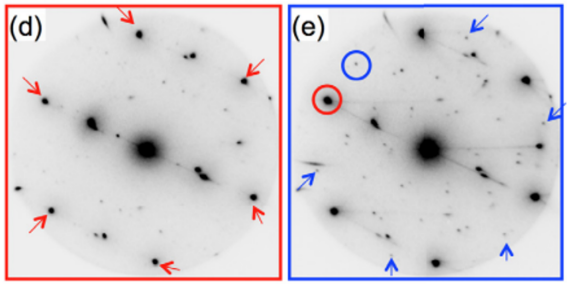

Figure 2.6: LEED on a single- and bilayer graphene. Left figure points out six corners of a honeycomb lattice in red, right figure points out another honeycomb lattice in blue, rotated 23° with lower intensity. Image used under a Creative Commons Attribution 3.0 Unported License. [24]

2.3 Transfer processes

One common method to transfer graphene is wet transfer. The copper foil with graphene on top is spin-coated with PMMA, copper is etched, and the PMMA/-

graphene sample is placed on a substrate and dried. In the last step, the PMMA is dissolved in acetone. The process is described by Kim et al. [25]. When the transfer is finished, the multilayers that grow closest to the copper foil are positioned closest to the substrate, as illustrated in Figure 1.1(c). The wet transfer process is shown in Figure 2.7. Here silicon is used as a final substrate.

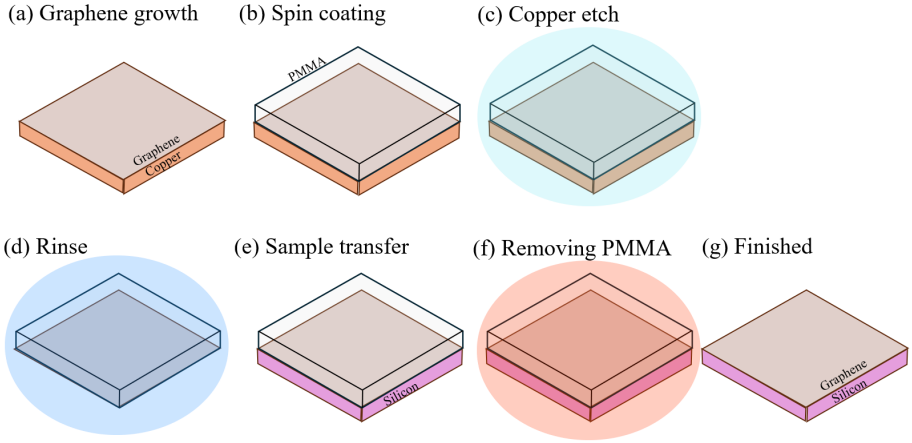

Figure 2.7: Wet transfer process: **(a)** CVD process, graphene is grown on copper foil, **(b)** copper foil are spin-coated with PMMA, **(c)** copper is etched, **(d)** sample is rinsed in DI water, **(e)** silicon is used as a final substrate, **(f)** PMMA is removed with acetone, and **(g)** graphene on silicon.

Khan et al. transferred graphene to a lamination foil [4]. Copper foil with graphene was laminated to lamination foil using an office laminator. This is followed by etching the copper foil, resulting in a lamination foil with graphene. Transferring graphene in this way eliminates the process of removing the spin-coated preliminary substrate. The patches that grow closest to the copper foil are positioned on top of the single-layer graphene instead of below. This is a direct transfer process. Figure 2.8 shows the lamination transfer process.

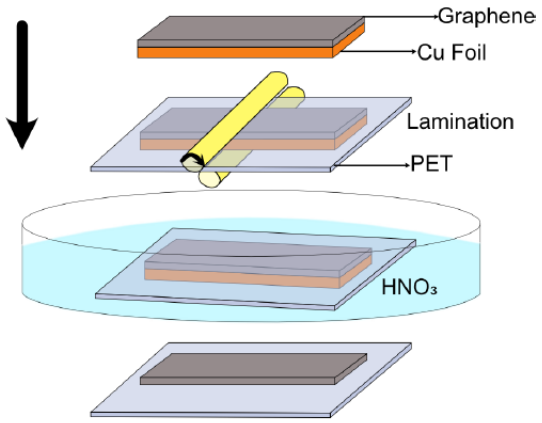

Figure 2.8: Process flow for graphene transfer from Cu foil to lamination foil. Image used under a Creative Commons Attribution 4.0 Unported License. [4]

In summary, besides the difference in the number of steps needed to transfer

graphene in the direct- and double-transfer process, the patches positions, relative to the graphene open surface, differ depending on what process is used. As described earlier, the patches grow closest to the copper foil in the CVD process. Therefore, the patches are positioned on top of the single-layer graphene after a direct-transfer process illustrated in Figure 2.9(a), and below the single-layer of graphene in a double-transfer process illustrated in Figure 2.9(b). The patches contours are outlined as continuous in Figure 2.9(a) because they are positioned on top. The patches contours are outlined as dashed in Figure 2.9(b) since they are positioned below the single layer of graphene.

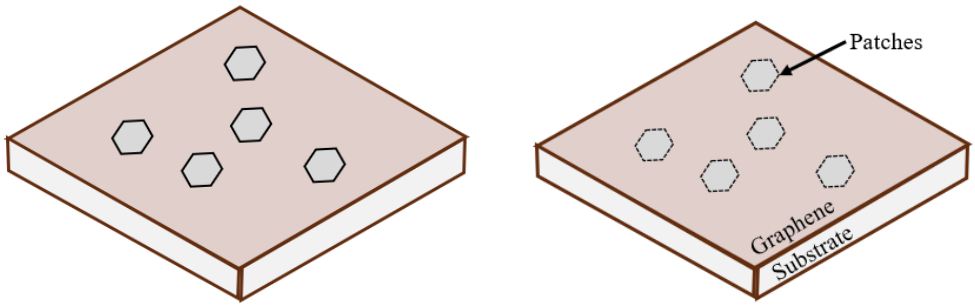

(a) **(b)**

Figure 2.9: Illustration of patches position. **(a)** Direct transfer of graphene, patches on top. **(b)** Double transfer of graphene, patches are positioned below the single layer.

When graphene is transferred with PMMA as a preliminary substrate in a wet transfer process, mobility decreases because of wrinkles and contamination from the transfer process. These factors reduce the charge carrier mean free path, which limits carrier mobility [18]. The final substrate used also plays a major role in defining mobility. Leong et al. also reported on the downside of using PMMA as a preliminary substrate in a wet transfer process [26]. It caused polymer contamination and wrinkling in the graphene. This study compares PMMA and paraffin. Paraffin has an alkane simple nonreactive structure, and they report that paraffin leaves less residue on graphene as it does not contain carbonyl (C=O), which can react with materials that are electrophiles or nucleophiles, i.e., materials that accept or donate electrons. It is also noted that paraffin has a lower surface energy than PMMA and that field effect transistors fabricated on paraffin-transferred graphene had almost zero Dirac voltage (no parasitic doping from residues). The mobility was four times higher than that of PMMA-transferred graphene.

Martins et al. did direct transfer to different substrates [27]. In this article, they did not measure the doping, only sheet resistance. They investigated transfer to different flexible substrates, not including PMMA as a middle step, i.e., direct transfer. They reported using hydrophobic substrates with low glass transition temperatures as the most efficient. Ren et al. also report improved qualities in graphene when directly transferring graphene [28]. In this report, the authors compare direct- and

double-transfer methods. They suggest that PMMA influences mobility and doping in the graphene. Reducing the unintentional doping that can occur after etching was studied. Hassanpour Amiri et al. etched the copper with $FeCl_3$, washed it in NH_3, and reported improved quality by doing so [29].

2.4 Scanning electron microscopy

Electron deflection by magnetic field was discovered during the 1890s. Since then, electron microscopy has become very popular. In Scanning Electron Microscopy, shortened as SEM, the image produced is based on the signals from an electron gun, shooting an electron beam with primary electrons at an energy level of 0.1-30 keV. The output signal is how the sample responds to being hit by this beam. Signals handled during SEM operations are Auger electrons, secondary electrons, back-scattered electrons, characteristic x-rays, and x-ray continuum. [30]

SEM studies result in greyscale images based on the efficiency of producing secondary electrons or backscattering electrons. The areas of the sample with higher conductivity are represented with a lighter color, and darker spots represent lower conductivity. When examining transferred graphene on plastic substrates, the darker regions would represent double- or multi-layer regions, and the lighter-grey monotonous region would be the single layer.

3

Material and method

This chapter describes the materials and methods used in this project. Graphene was grown on copper foil and transferred to substrates using different adhesives. Adhesives were also applied on top of samples, quality was measured, and morphology was examined in SEM.

3.1 Adhesives with high melting temperature

This project used a quickly curing epoxy resin from REXXAN and EPO-TEK 730 from Epoxy Technology as adhesives. REXXAN was bought from the food store chain Lidl; getting a datasheet was impossible. However, it contains Bisphenol F diglycidyl ether, which is shortened to DGEBF. It was estimated to have a degradation temperature of 383°C [31]. GA Lindberg kindly provided EPO-TEK 730; datasheets are available. These adhesives can withstand temperatures >100°C and can theoretically be used in photolithography. Important characteristics of the glues are summarized in Table 3.1. EPO-TEK 730 has an alternative cure; 24 hours at 23°C, but the supplier does not guarantee listed properties in their data sheets for this process. Samples glued with EPO-TEK 730 were dried at 23°C before being moved to an oven for heating since pressure and heat could not be applied simultaneously.

Table 3.1: Collection of adhesives examined in this thesis.

	T_{degr} [°C]	Cure
REXXAN	383	24 hours at 23°C
EPO-TEK 730	343	2 hours at 80°C (or 24 hours at 23°C)

3.2 Chemical vapor deposition

Graphene was grown in an MTI OTF-1200X model tube-in-tube CVD system. A copper foil, 25 µm thick, was cut into 10 cm wide pieces and long enough to cover the full circumference of the inner quartz tube in the furnace.[1] Before the copper foil was mounted on the tube, it was immersed in acetic acid for a few minutes to

[1] Image of the system used is found in Appendix A.1

remove oxides from the surface. The foil was then cleansed in DI water and blow-dried with nitrogen. The foil was wrapped around the tube, and the meeting edges were folded. The foil was placed at the center of the furnace, and the tube was mounted inside the outer tube.

The recipe for growth includes a ramp-up time of 50 min to 1050°C, followed by 30 min annealing, combined with a flow of 10 sccm H_2 and 50 sccm Ar. After this, the temperature was decreased to the growth temperature, and methane (5% CH_4 diluted in Ar) was added. Three growth processes were executed, with growth temperature, T_{gr}, growth time, t_{gr}, and methane flow rate, summarized in Table 3.2. The different growths are named after the date they were performed.

Table 3.2: Growth recipes.

	T_{gr} [°C]	t_{gr} [min]	Methane [sccm]
February 1	980	15	20
February 15	1000	15	10
February 21	1000	30	15

When growth was finished, the temperature was rapidly decreased to room temperature. The copper foil was dismounted from the tube and cut in half. The side closest to the gas inlet was marked. A slice of the copper foil was divided into 6 samples to examine the graphene growth in the quartz tube. Sample number 1 was closest to the gas inlet. Samples 1 to 6 are schematically shown in Figure 3.1. A high-quality CVD graphene, referred to as the bought graphene, was bought from Graphenea to benchmark the CVD grown graphene.

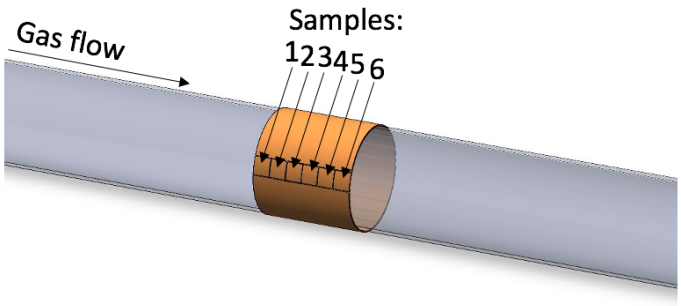

Figure 3.1: Copper foil mounted on quartz tube. Sample number 1 is closest to the gas inlet.

3.3 Removal of copper

Copper can be removed in several ways; chemical etching and so-called bubbling delamination are used here. Chemical etching was done either in nitric acid, HNO_3 30% or iron(III) chloride, $FeCl_3$ 50%. The samples were placed in the solution for approximately 5 minutes and 120 minutes, respectively. Regardless of the removal

method, the samples were washed in DI water afterward and dried in a nitrogen flow. Additionally, the samples could be washed in ethanol for 5 minutes. When using HNO_3, copper(II) nitrate is created. When using $FeCl_3$, FeCu and Cl_3 are created as substitutes. The reactions can be described as follows:

$$3Cu + 8HNO_3 \Rightarrow 3Cu(NO_3)_2 + 2NO + 4H_2O \tag{3.1}$$

$$Cu + FeCl_3 \Rightarrow FeCu + Cl_3 \tag{3.2}$$

Bubbling delamination was performed by applying a current of 0.5 A between the sample as the cathode and a plate of platinum as an anode. The sample and plate were in a beaker with 0.25 M of NaOH for 3 minutes when the current was applied. During bubbling delamination, the negatively charged cathode produces hydrogen [32]. This delaminates the copper from the graphene while the adhesive layer still sticks the graphene to the substrate. The reaction formula is:

$$2H_2O(aq) + 2e^- \Rightarrow H_2(g) + 2OH^-(aq) \tag{3.3}$$

3.4 Transfer to substrates

This section describes direct- and double-transfer with adhesives mentioned in section 3.1. Graphene was transferred using EVA/PET (lamination foil) according to Khan et al.[4]. Direct transfer means that the patches are positioned on top of single-layer graphene as illustrated in Figure 3.2(a). Here the patches are marked in black since they are positioned on top of single layer graphene. Double transfer means that the patches are positioned below single-layer graphene as illustrated in Figure 3.2(b). Here the single layer is marked in black since it is positioned on top of the patches.

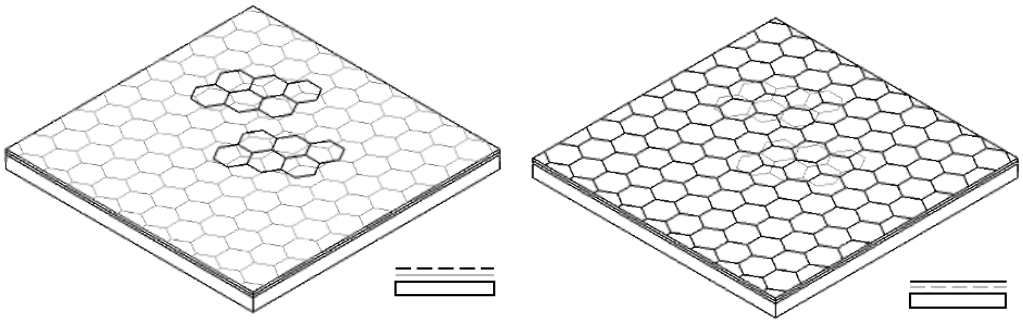

(a) **(b)**

Figure 3.2: Illustration of patches position. **(a)** Direct transfer of graphene, patches on top. **(b)** Double transfer of graphene, patches are positioned below the single layer.

3.4.1 Direct transfer

Graphene transfer from copper foil started with mixing epoxy components; this was done by mixing equal parts according to supplier information. The mixing tool used was a small toothpick in a small plastic beaker. The adhesive was after that applied to a plastic substrate[2]. The substrate with the adhesive was then placed on a flat surface. A small piece of copper with graphene, ca. 1 cm^2, was placed on top with graphene pointing towards the adhesive. A small amount of pressure was applied during the curing time.[3] The copper foil was in the last step removed; see details in section 3.3. Patches are now oriented on top of the monolayer, as illustrated in Figure 3.2(a).

3.4.2 Double transfer

Graphene was first transferred to a preliminary substrate. Then, a plastic substrate[2] with adhesive was applied on top of the graphene, and the preliminary substrate was removed. Parafilm was used as a preliminary substrate. To transfer graphene to parafilm, the copper foil was heated to 50°C in a small chamber with nitrogen flow.[3] Parafilm was heated to 50°C on the chamber's lid since this provided a flat surface for sample preparation. The copper foil was placed on the parafilm with graphene pointing to the parafilm, followed by gently rolling with a rubber roller.[3] The sample was removed from the hot lid, and copper was etched in HNO_3, see details in section 3.3. The preliminary substrate has graphene with patches on top, illustrated in Figure 3.2(a).

Epoxy components were mixed according to supplier information and applied to a plastic substrate[2]. The preliminary substrate (Figure 3.3(a)) was applied on top of the substrate with adhesive (Figure 3.3(b)), and a small pressure was added during the curing time (Figure 3.3(c))[3]. To peel off the preliminary substrates, parafilm was heated to 50°C and gently peeled off (Figure 3.3(c)). Patches are now below the graphene monolayer on the sample, shown in 3.2(b).

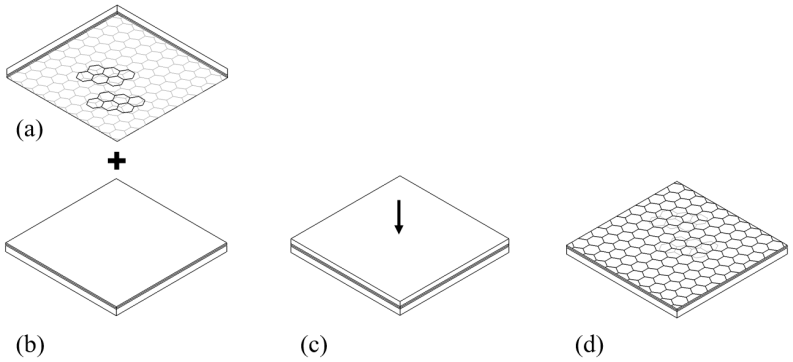

Figure 3.3: **(a)** Preliminary substrate with graphene, **(b)** plastic substrate with adhesive, **(c)** pressure added during curing time, **(d)** preliminary substrate peeled off, patches are positioned below single-layer graphene, shown in 3.2(b).

[2]PEEK etc.

[3]The transfer equipment used is collected in Appendix A.2

3.5 Top gluing

The impact of the adhesive on the graphene was evaluated by applying glue on top. In this thesis, this process is referred to as top gluing. When top gluing a sample, the other side of the graphene that does not face the substrate is also covered with adhesive, i.e., creating a sandwich with the graphene in the middle.

Graphene was directly transferred with REXXAN and EPO-TEK 730, Figure 3.4(a). Before applying glue on top, the samples were shaped, leaving surfaces for the probes at the corners of the sample, Figure 3.4(b). The adhesives were applied on top, Figure 3.4(c). The top glue was cured for 24 hours at 23°C.

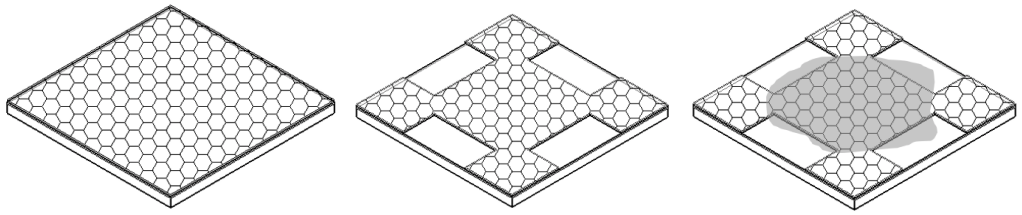

(a) **(b)** **(c)**

Figure 3.4: The samples **(a)** right after copper is removed, **(b)** when the surface was shaped, and **(c)** when glue was applied on top.

3.6 Characteristics measurements

The samples were characterized using SEM and electrical measurements. The SEM tool used is Zeiss Supra 55 - EDX. Images were taken at a working distance of 5 mm at 7 kV with 1000X, 5000X, and 10000X magnification. Subsequently, the existence of multilayers could be examined.

The electrical properties of the samples were characterized by conducting resistivity and Hall effect measurements using VDP's method. The sample was mounted in a small rigg where four probes were attached to each corner of the sample.[4] VDP's measurements resulted in sheet resistance, R_s. The carrier concentration, n, could be determined with hall measurements. With these two parameters, the mobility was calculated as:

$$\mu = 1/(qR_s n) \tag{3.4}$$

[4]The measurement equipment used is collected in Appendix A.3

4

Results

This chapter presents the results of CVD grown graphene, which includes analysis in SEM and analysis of the sample's position in the CVD chamber. It also presents direct- and double-transfer processes and the adhesive's impact on the graphene properties. Improvements for future work are also presented.

4.1 Analysis of CVD grown graphene in SEM

SEM images from growth on February 1, February 15, and February 21 are summarized in Figure 4.1. At the lowest magnification, 1000X, it is seen that there are multilayers of graphene in all three growths. It is also visible that the growth somewhat follows lines, which are assumed to be from the copper foil or the induced flow of gases in the chamber. The orientations of how the samples were positioned during the CVD were not followed in the SEM; the direction or the cause of the lines can not be determined.

Analyzing the images where the magnification is increased, it is seen that there are fewer multilayers at the latest growth, Figure 4.1(c). Fewer multilayers are beneficial for improving quality and T_{gr} could be a factor. In Figure 4.1(a), T_{gr} is lower, and the flow rate of CH_4 is higher. In Figure 4.1(b), T_{gr} was raised, and the flow rate of CH_4 was lowered. Thereafter, t_{gr} was increased in Figure 4.1(c), and the flow rate of CH_4 was increased. The input parameters that differ are summarized at the top of Figure 4.1.

As assumed, the bought graphene exhibited significantly fewer patches, as demonstrated in the SEM image shown in Figure 4.2. Previous research has claimed that graphene initially grows from the center of the copper grains [20][23][24], this is not visible here. Yu et al. discussed placing seeds on copper to initiate growth [18], and it is quite unlikely from Figure 4.2 that this was their approach since the patches are randomly distributed over the surface. Another approach for reaching high-quality graphene is to have less methane at the beginning of t_{gr}, to initialize growth. This could have been the strategy for processing this bought graphene since the patches are randomly placed. Patches do not seem to grow along any lines from the copper foil as the growth did in Figure 4.1.

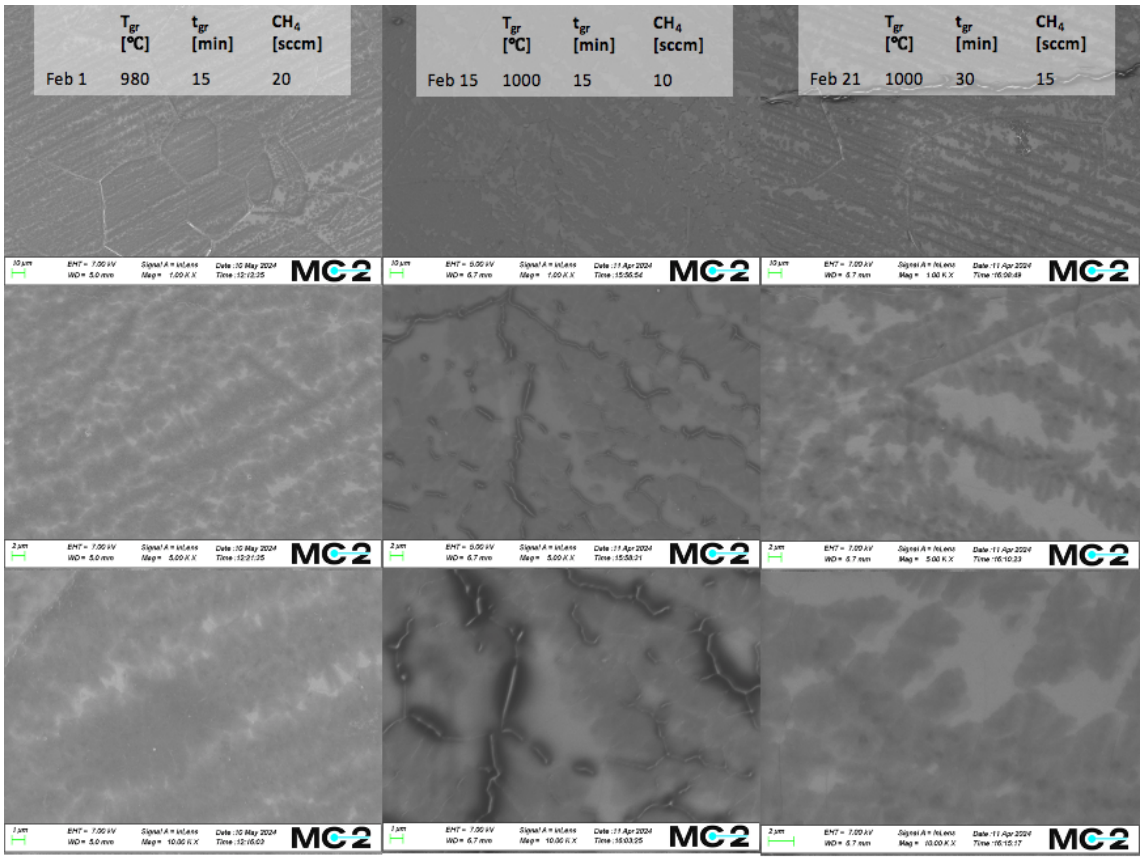

Figure 4.1: SEM images of growth on **(a)** February 1, **(b)** February 15, and **(c)** February 21. Graphene was transferred to lamination foil, copper was etched in HNO_3. Images collected at, from top to bottom; 1000X, 5000X, and 10000X.

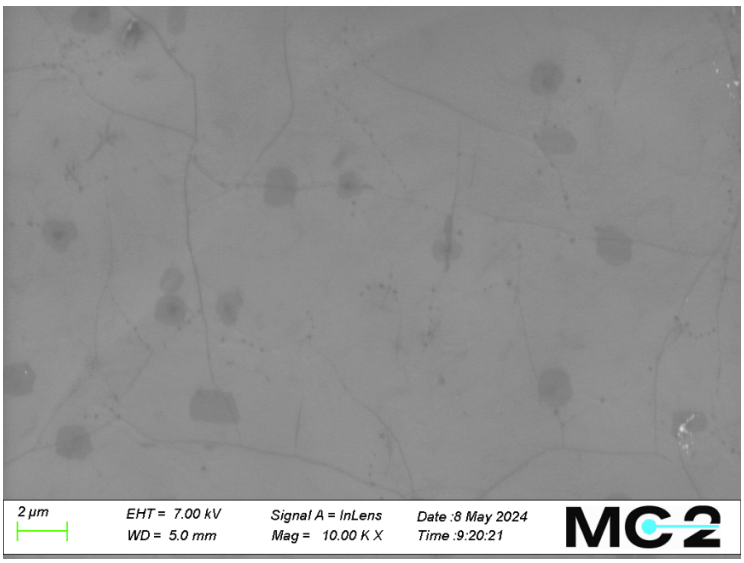

Figure 4.2: SEM image of bought graphene transferred to lamination foil, copper was etched in HNO_3. Image collected at 10000X.

4.2 Analysis growth in CVD

The samples grown on February 1 had mobility of ca. 400 - 500 $cm^2/(V{\cdot}s)$, samples grown on February 15 had mobility of ca. 300 - 700 $cm^2/(V{\cdot}s)$, and graphene grown on February 21 had mobility of ca. 900 - 1200 $cm^2/(V{\cdot}s)$. All numbers collected are from graphene directly transferred to lamination foil. Characteristics of samples 1-6 for growth on February 1, February 15, and February 21 are shown in Table 4.1, Table 4.2 and Table 4.3 respectively.[1] Out of the 6 samples from a stripe, the best quality was achieved for samples 3 or 4, i.e., at the center of the 10 cm wide stripe that was wrapped around the quartz tube. Also, it is seen that the samples closer to the gas inlet had slightly higher mobility, i.e., samples 1-3 had higher mobility compared to samples 4-6.

Table 4.1: Properties of graphene grown on February 1 and transferred to EVA/PET foil. Copper etched in HNO_3, samples washed in ethanol for 5 minutes and washed in DI water.

Position	1	2	3	4	5	6
R_s [$\Omega/\square$]	1290	1590	1590	1450	1840	1660
μ [$cm^2/(V{\cdot}s)$]	526	485	451	446	463	415
R_H [$\Omega/\square$]	10.7	12.1	11.3	10.2	13.4	10.9
n [10^{12} cm^{-2}]	9.2	8.1	8.7	9.7	7.3	9.0

Table 4.2: Properties of graphene grown on February 15 and transferred to EVA/PET foil. Copper etched in HNO_3, samples washed in ethanol for 5 minutes and washed in DI water.

Position	1	2	3	4	5	6
R_s [$\Omega/\square$]	10000	8930	7350	12000	20000	12000
μ [$cm^2/(V{\cdot}s)$]	441	570	716	341	284	363
R_H [$\Omega/\square$]	71.0	79.0	82.7	62.0	90.0	68.5
n [10^{12} cm^{-2}]	1.3	1.2	1.2	1.5	1.0	1.4

Table 4.3: Properties of graphene grown on February 21 and transferred to EVA/PET foil. Copper etched in HNO_3, samples washed in ethanol for 5 minutes and washed in DI water.

Position	1	2	3	4	5	6
R_s [$\Omega/\square$]	2460	2840	2450	2670	3240	2770
μ [$cm^2/(V{\cdot}s)$]	1020	1040	1240	1140	953	928
R_H [$\Omega/\square$]	39.5	46.4	47.9	48.0	48.5	40.4
n [10^{12} cm^{-2}]	2.5	2.1	2.0	2.0	2.0	2.4

[1]The samples in Table 4.2 and Table 4.3 were also annealed at 60°C, but showed no direct improvement. This could be because the samples were washed in ethanol for 5 minutes, which was found to also improve the mobility of transferred graphene. Data summarized in Appendix B.1.

When copper foil was placed at the center of the quartz tube, and the oven was placed centric over the copper foil, these actions were made with eye measurement. Since all three growths showed improved qualities closer to the gas inlet, it can be assumed that it is the center of copper foil that creates the best quality graphene. There could be several reasons for this outcome.

- **Cold-rolled foil parameters**, such as curved rollers, are commonly used in milling operations to compensate for the force applied by the roller. Adding annealing, it is not certain how the thickness differs along the foil when growth starts. Yilmaz et al. report that the thickness of copper foil plays an important role in the characteristics of graphene [19].
- **The temperature of gases** can differ along the copper foil since the gas flow comes from one side and, therefore, does not have the same temperature when it reaches the other side of the copper foil.
- **More carbon atoms** are present further away from the gas inlet because the precursor gas can interact with the copper foil for a longer period of time, forming more patches and resulting in lower quality.
- **Non-uniform temperature** of the foil during growth and cool-down causes larger radiation losses at the edges that are closer to the ends of the furnace.

4.3 Direct- and double transfer

As described in Section 4.2, the quality of graphene varies depending on what position, 1-6, a sample is cut from the copper foil. Further, these positions were not followed in this project, but the quality of graphene should lay within the range of mobilities mentioned in section 4.2. During the direct transfer of graphene, all samples showed p-doping no matter what glue was used. Also reported in previous studies, e.g. Khan et al. [4]. Direct-transferred graphene on parafilm also results in p-doped graphene, shown in Table 4.4.

The result from the direct transfer with REXXAN and EPO-TEK 730 is shown in Table 4.5. It is seen that transferring graphene on REXXAN results in the same range of mobility as the EVA/PET foil. The same is true for graphene transferred to parafilm. As mentioned in section 3.1, EPO-TEK 730 could be cured for 24 hours at 23°C, but the supplier does not guarantee stated properties in the data sheet by doing so. To successfully double transfer with EPO-TEK 730, it could only be cured at this low temperature since parafilm can not be cured at 80°C. The result of this type of cure is visible in Table 4.5. One can assume that this EPO-TEK 730 was not cured properly and, therefore, does not fall within the range of mobility that EVA/PET-transferred graphene has. In Table 4.6, the results from the double transfer are presented.

Table 4.4: Results from direct transfer on parafilm. Copper etched in HNO_3.

	Parafilm
R_s [$\Omega/\square$]	853
μ [$cm^2/(V{\cdot}s)$]	1110
R_H [$\Omega/\square$]	14.8
n [10^{12} cm^{-2}]	6.6

Table 4.5: Direct transfer to REXXAN (A) and EPO-TEK 730 (B). Copper was etched in HNO_3. Patches are on top of monolayer, seen in Figure 4.3(a).

	A	B
R_s [$\Omega/\square$]	2360	388
μ [$cm^2/(V{\cdot}s)$]	1160	574
R_H [$\Omega/\square$]	42.8	3.5
n [10^{12} cm^{-2}]	2.3	28.0

Table 4.6: Double transfer with parafilm as preliminary substrate and graphene transferred to REXXAN (A) and EPO-TEK 730 (B). Patches are below monolayer, seen in Figure 4.3(b).

	A	B
R_s [$\Omega/\square$]	4830	4290
μ [$cm^2/(V{\cdot}s)$]	-399	-280
R_H [$\Omega/\square$]	-30.3	-18.8
n [10^{12} cm^{-2}]	-3.2	-5.2

The directly transferred graphene has its patches on top and is p-doped for all samples tested, shown in Figure 4.3(a). The double-transferred graphene has its patches below the single-layer graphene and is n-doped, Figure 4.3(b). The double transfer was also tested with two other types of adhesives, Araldite and EPO-TEK 323, which will not be discussed further. These also got n-doped results. Data from these transfers are found in Appendix C.1.

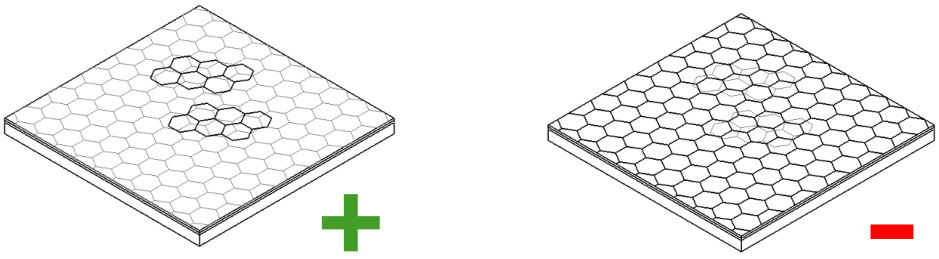

(a) **(b)**

Figure 4.3: Dark honeycomb structure represents top layer of graphene. **(a)** Directly transferred graphene is p-doped with patches on top and **(b)** double transferred graphene is n-doped; patches are below monolayer.

4.4 Adhesive's impact on graphene

The effect of shaping the samples, illustrated in Figure 3.4, was examined in Appendix D.1. It is seen that the quality of the shaped samples is better. When measuring some samples, poor contacts were received between the probes and the

graphene; the results from these samples are not shown in the tables.[2] This section is divided into three subsections. First, the adhesive's impact on graphene with many patches i.e., February 21, is presented. Then, the adhesive's impact on graphene with few patches, i.e., the bought graphene, is presented. Lastly, a discussion of differences between graphene with many patches and few patches is adopted.

4.4.1 Graphene with many patches

Table 4.7 shows the results when directly transferring graphene with many patches, i.e. graphene grown on February 21, to REXXAN and EPO-TEK 730, followed by applying glue on top of the samples. The upper part of the table represents the samples before having glue applied on top of graphene, i.e., samples illustrated in Figure 3.4(b). The bottom part of Table 4.7 represents the results after the glue has been applied on top, as in Figure 3.4(c). EPO-TEK 730 was here cured for 2 hours at 80°C. Mobility is now in the same range as for the direct transfer on EVA/PET. There is a higher mobility, μ, and lower carrier concentration, n, when using $FeCl_3$. This could be because $FeCl_3$ is not as strong etchant as HNO_3. When top glue was applied, the sheet resistance increased for all samples except for one of the B/B samples, which decreased by -16%; this could be an error sample since it has been proven to be positive in other samples, e.g. in Appendix D.1. It is seen that the carrier concentration decreased no matter which glue was applied on the top. Therefore, Δn has a negative sign. We can conclude that the top glue induced doping in a negative direction, but the overall doping can be both n and p, i.e., μ, R_H and n in the bottom part of Table 4.7 can both have negative and positive signs.

Table 4.7: Top gluing on direct transferred graphene grown on February 21, REXXAN (A) and EPO-TEK 730 (B). Copper etched in HNO_3 or $FeCl_3$.

		HNO_3				$FeCl_3$			
Fig. 3.4(b)		A/-	A/-	B/-	B/-	A/-	A/-	B/-	B/-
	R_s [Ω/□]	303	261	215	209	1310	865	682	639
	μ [cm^2/(V·s)]	748	1080	1030	1060	1430	877	1660	1680
	R_H [Ω/□]	3.6	4.5	3.5	3.5	29.5	11.9	17.8	16.9
	n [10^{12} cm^{-2}]	27.5	22.0	28.0	28.1	3.3	8.2	5.5	5.8
Fig. 3.4(c)		A/A	A/B	B/B	B/A	A/A	A/B	B/B	B/A
	R_s [Ω/□]	815	826	685	263	4300	1960	574	1810
	μ [cm^2/(V·s)]	1120	-564	-1250	1110	674	-357	-1530	2690
	R_H [Ω/□]	14.4	-7.3	-13.4	4.6	45.5	-11.0	-13.8	76.4
	n [10^{12} cm^{-2}]	6.8	-13.4	-7.3	21.4	2.2	-8.9	-7.1	1.3
	ΔR_s [%]	+169	+216	+219	+26	+231	+127	-16	+183
	Δn [%]	-75	-161	-126	-24	-33	-209	-229	-78

If one only considers the overall doping after applying glue on top, one might conclude that the adhesive used as the top glue causes the doping to reach negative val-

[2]Silver glue was used in an attempt to improve contact, seen in Appendix D.2. It shows that silver glue did not improve contacts.

ues on the carrier concentration, n. This would mean that applying EPO-TEK 730 on top will always result in graphene with n-doped qualities. Similarly, REXXAN would always produce p-doped graphene, regardless of the adhesive used during the direct transfer. However, this was proven wrong when REXXAN was applied to directly transferred graphene on EVA. This sample resulted in n-doped graphene. Out of curiosity, other glues[3] were tested as top glues, resulting in n-doped graphene when EVA was used as the adhesive for direct transfer. Data supporting this can be found in Appendix E.1. The overall doping after applying glue on top depends on; 1) the existing doping level in the samples, 2) the "doping-effectiveness" of the adhesive applied on top, and 3) the area that is covered by adhesive on the sample. Other glues[3] were also applied to directly transferred graphene on REXXAN and EPO-TEK 730. Data are available in Appendix E.2. The carrier concentration is initially higher because the samples were not washed in ethanol. When the glue is applied on top, all samples get decreased carrier concentrations, but not all reach negative values, i.e., not all became n-doped graphene. Mobility was calculated as described in Equation 3.4, where the carrier concentration is in the denominator. Lower value of carrier concentration results in higher mobility. Since the carrier concentration can change sign, the absolute value of carrier concentration is important to evaluate before- and after applying glue on top. This is demonstrated in Figure 4.4. It is seen that the samples that were etched with HNO_3 received higher carrier concentration, while the samples etched in $FeCl_3$ did not get as high carrier concentration. For the samples that were etched in HNO_3, the columns are shorter after applying glue on top i.e., the absolute value of carrier concentration decreased. This is partially true for $FeCl_3$ as well, but the A/B and B/B columns are almost of equal height. But here, it is clear that the B/A combination got a smaller column, and this is also the highest mobility achieved for graphene grown in this study while testing all top gluing combos. B/- reached a mobility of 1680 $cm^2/(V{\cdot}s)$ and B/A 2690 $cm^2/(V{\cdot}s)$. It can be concluded that the absolute value of the carrier concentration decreases when glue is applied on top, leading to higher mobility. The difference between etching in HNO_3 and $FeCl_3$ is that the carrier concentration is generally lower for the samples etched in $FeCl_3$.

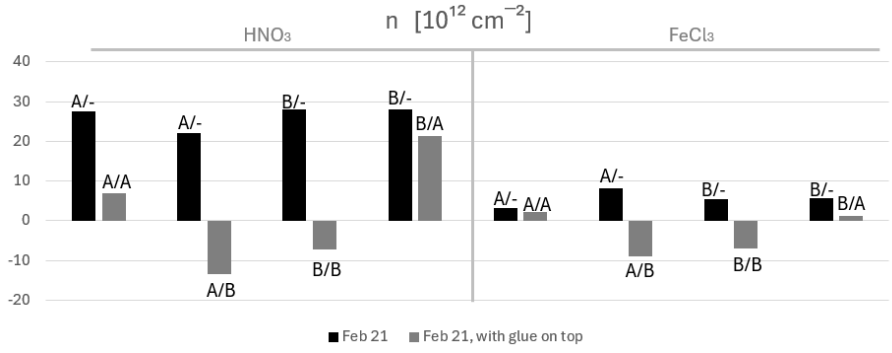

Figure 4.4: Carrier concentration, n, for graphene grown on February 21, plotted as a bar chart, data from Table 4.7.

[3]Araldite and contact glue

4.4.2 Graphene with few patches

The same set of samples was created for graphene with few patches, i.e. the bought graphene. The results are presented in Table 4.8. It is evident that the effect of the etchant is still present, resulting in generally lower carrier concentrations in the samples etched in $FeCl_3$. Generally, we observe higher mobility for graphene transferred on REXXAN and lower mobility for graphene transferred on EPO-TEK 730. When applying adhesive on top, the sheet resistance increased for all samples etched in HNO_3 and generally decreased for samples etched in $FeCl_3$. Carrier concentration decreased for all samples except for the A/A combination for both types of etchants. These samples instead became p-doped with increasing carrier concentration. This was tested on two more samples where bought graphene was directly transferred with REXXAN and etched in HNO_3, and then REXXAN was also applied on top. This did not result in p-doped samples, Δn was -116% and -118%. Data in Appendix E.3. The same test was not executed for A/A in $FeCl_3$, but it was here assumed that the carrier concentration would decrease here as well.

When etching the copper from the samples in Table 4.8 in HNO_3, the samples got increased R_s when applying glue on top, but the opposite happened to the same samples etched in $FeCl_3$. Therefore, the selected method for removing copper affects the result when glue is applied to the samples in terms of R_s.

Table 4.8: Top gluing on direct transferred bought graphene, REXXAN (A) and EPO-TEK 730 (B). Copper etched in HNO_3 or $FeCl_3$.

		HNO_3				$FeCl_3$			
Fig. 3.4b		A/-	A/-	B/-	B/-	A/-	A/-	B/-	B/-
	R_s [Ω/□]	708	653	1800	1840	763	963	13720	2060
	μ [cm^2/(V·s)]	2910	2210	427	375	1900	2400	752	1260
	R_H [Ω/□]	32.4	22.7	12.1	10.8	22.8	36.4	162	40.8
	n [10^{12} cm^{-2}]	3.0	4.3	8.1	9.1	4.3	2.7	0.6	2.4
Fig. 3.4c		A/A	A/B	B/B	B/A	A/A	A/B	B/B	B/A
	R_s [Ω/□]	2490	680	5730	5820	2140	504	4530	1310
	μ [cm^2/(V·s)]	385	-2500	-284	1670	585	-2580	-432	-998
	R_H [Ω/□]	15.0	-26.7	-25.5	153.0	19.6	-20.4	-30.7	-20.6
	n [10^{12} cm^{-2}]	6.5	-3.7	-3.8	0.6	5.0	-4.8	-3.2	-4.8
	ΔR_s [%]	+252	+4	+218	+216	+180	-48	-67	-36
	Δn [%]	+117	-186	-147	-93	+16	-278	-633	-300

In Figure 4.5, the value of n before- and after applying glue on top is shown for the bought graphene. Besides the A/A combination, which was discussed above, where there could be errors, the other data for the samples etched in HNO_3 presents smaller column heights when applying glue on top of the samples. This is, however, not true for the samples etched in $FeCl_3$. Here it seems like the absolute value of carrier concentration actually is larger after applying glue on top, and therefore promotes lower mobility according to Equation 3.4. It concludes that the graphene with few patches gets more n-doped than the graphene with many patches and does

not promote increased mobility when applying glue on top.

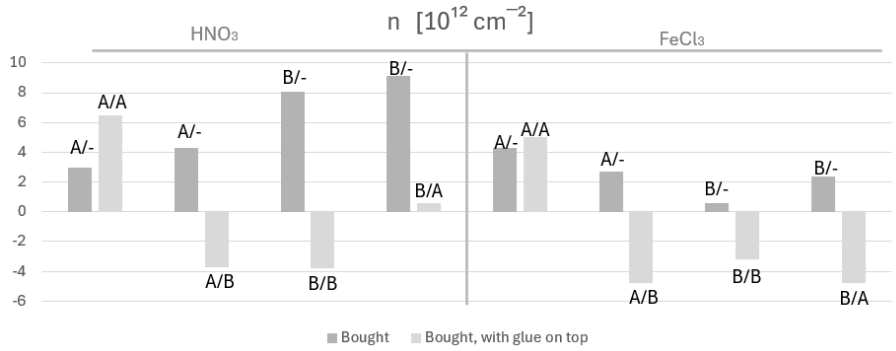

Figure 4.5: Carrier concentration, n, for bought graphene plotted as a bar chart, data from Table 4.8.

4.4.2.1 Bubbling delamination

Bubbling delamination was only successful for the bought graphene, when using REXXAN as an adhesive. The graphene grown on February 21 is assumed to have too rough copper foil for the method to be successful. Two samples were directly transferred with REXXAN, and copper was removed with bubbling delamination. The effect of washing in ethanol for 5 minutes is summarized in Table 4.9. It is evident here that mobility and carrier concentration decreased while sheet resistance increased. These samples underwent the same tests involving the application of adhesive on top of the graphene, with data available in Table 4.10. The only difference from Table 4.8 is that in Table 4.10, the removal of copper was done using bubbling delamination.

Table 4.9: Direct transferred bought graphene on REXXAN, copper removed with bubbling delamination.
The lower part of the table shows samples after being washed for 5 minutes in ethanol.

		#1	#2
NO WASH	R_s [Ω/□]	4510	3340
	μ [cm^2/(V·s)]	1060	1690
	R_H [Ω/□]	72.1	88.5
	n [10^{12} cm^{-2}]	1.3	1.1
WASH	R_s [Ω/□]	11650	6040
	μ [cm^2/(V·s)]	965	1320
	R_H [Ω/□]	176.5	124.9
	n [10^{12} cm^{-2}]	0.6	0.8

Table 4.10: Top gluing on direct transferred bought graphene. REXXAN (A) and EPO-TEK 730 (B). Copper was removed with bubbling delamination.

		A/-	A/-
Fig. 3.4b	R_s [Ω/□]	1290	1260
	μ [cm^2/(V·s)]	2970	2850
	R_H [Ω/□]	60.0	58.3
	n [10^{12} cm^{-2}]	1.6	1.7
		A/A	A/B
Fig. 3.4c	R_s [Ω/□]	793	435
	μ [cm^2/(V·s)]	-3210	-2860
	R_H [Ω/□]	-39.9	-19.6
	n [10^{12} cm^{-2}]	-2.5	-5.0
	ΔR_s	-39 %	-65 %
	Δn	-256 %	-394 %

4.4.3 Comparison; many patches and few patches

The difference between the results in Table 4.7, Table 4.8 and Table 4.10; seems to come from the different density of patches, seen in Figure 4.6, and the method used to remove copper. HNO_3 is the most aggressive etchant, and bubbling delamination is the gentlest. As described in Equation 3.4, the mobility is calculated with R_s and n as input parameters in the denominator. Therefore, small numbers on R_s and n correlate to higher mobility.

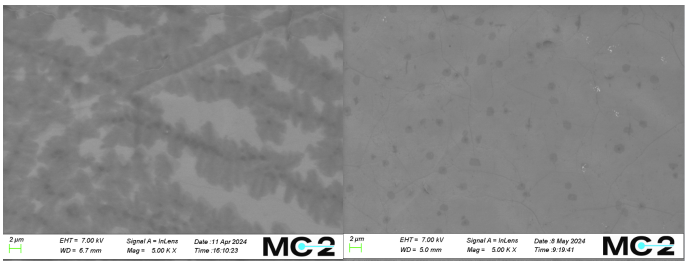

(a) **(b)**

Figure 4.6: **(a)** February 1 growth and **(b)** bought graphene. 5000X magnification.

The changes in sheet resistance are visible in Figure 4.7. For the graphene grown on February 21, the sheet resistance generally increased when top glue was applied on samples when copper was etched with HNO_3 and $FeCl_3$. The B/B combination for the $FeCl_3$ etchant deviates from this trend, as discussed in section 4.4.1. There are no SEM images to confirm the density of patches in this sample. For the bought graphene, sheet resistance increases when using a stronger etchant (HNO_3) but tends to decrease when using softer etchants ($FeCl_3$ and bubbling). The A/A combination for the $FeCl_3$ etchant deviates from this trend, as discussed in section 4.4.2. There are no SEM images to confirm the density of patches in this sample either.

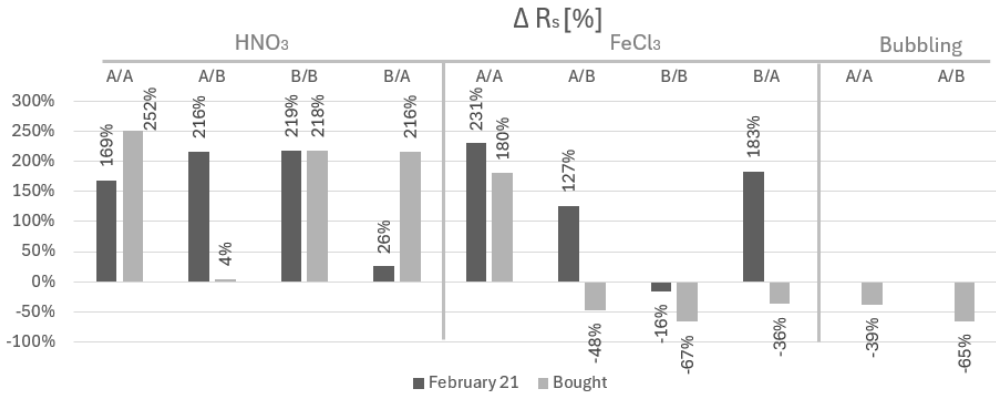

Figure 4.7: ΔR_s [%] after applying glue on top, for all combinations.

The percentage change of carrier concentration is shown in Figure 4.8. It is seen that the carrier concentration decreased for all samples after top gluing, as previously mentioned. This was true for both types of etchants except for the A/A

combinations with the bought graphene. This was further tested with two samples etched in HNO_3, which resulted in decreased carrier concentrations of -116% and -118% (Appendix E.3). A/A combination for the bought graphene with HNO_3 and $FeCl_3$ are therefore assumed to have some unidentified error. It can be concluded that the carrier concentration decreases more when using a milder etchant ($FeCl_3$).

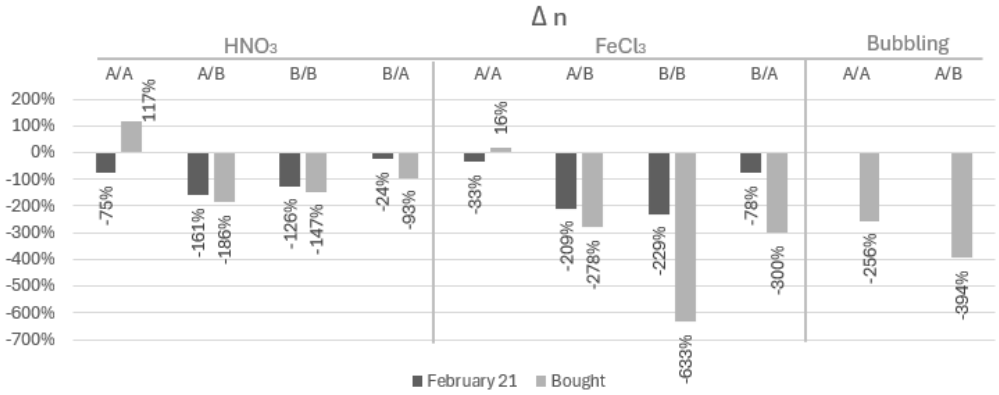

Figure 4.8: Δn [%] after applying glue on top, for all combinations.

For the graphene with many patches, low absolute values of n was achieved by etching in $FeCl_3$. Even lower values can be achieved by applying glue on top (Figure 4.4). The best combination found in this experiment is the B/A combination for the copper etched in $FeCl_3$ (1680 $cm^2/(V \cdot s)$, Table 4.7). Applying glue on top of graphene with many patches tends to increase R_s while using both types of etchants to remove copper (February 21, Figure 4.7).

For the graphene with fewer patches, low absolute values of n, when using HNO_3, are achieved by applying glue on top. But when using a softer etchant, like $FeCl_3$, the absolute value of n increases when applying glue on top (Figure 4.5). Low values of R_s are achieved by using $FeCl_3$ or bubbling delamination and applying glue on top of these samples (Bought, Figure 4.7).

4.5 Suggestion for future work

In the future, within this specific subject, by further improving the recipe for graphene growth in the MTI OTF-1200X model tube-in-tube CVD system, the outcome of this project suggests the use of $FeCl_3$ to remove the copper foil. While doing this, lower carrier concentration can be expected (Figure 4.4), and by applying glue on top carrier concentration could decrease even further. R_s would, however, increase, but if growth is improved and fewer patches are present, R_s should eventually not increase and instead decrease as it did for the bought graphene (Figure 4.7).

During this work, some points for improvement were identified.

(1.) **Shaping** the samples was in this project done by hand. I.e., samples were cut in square sizes, and the shaping in Figure 3.4(b) was done by hand. If the square samples instead were to be created with a punch tool or similar, then the shaping could also be done with a similar process. This would provide an area of equal size when doing the electrical measurements. This would also increase the number of examined samples in future studies since less time would be spent on cutting and shaping the samples.

(2.) **Mixing** of epoxy glues has been done manually with eye measuring the amount of each part during this project. Mixing was done carefully with a toothpick not to induce air bubbles in the adhesive layer. A more precise mixing could be achieved with a mixing nozzle or similar.

(3.) **The amount of applied top glue** was not measured. As a suggestion, the area that the top glue covers should be controlled in the future since it could affect doping. The top glue that covers larger areas on the samples affects graphene more than the samples where the top glue covers smaller areas. Alternatively, if the samples have the exact same size as the suggested improvement in point (1.), the weight or volume of applied top glue could be measured instead.

(4.) **Heat and pressure was not available simultaneously.** The glues that required heat to cure in this study were first dried at room temperature for 24 hours. This was due to the fact that pressure and heat could not be applied at the same time with the equipment available for this study. Applying both heat and pressure at the same time could affect the result. A suggestion is to modify the transfer equipment in Appendix A.2, Figure A.2, so the large bottom plate could be heated and the wooden bars replaced with metallic ones. In that way, heat could be applied to the samples simultaneously with pressure. Improved results could potentially be received, but also a lot of time would be saved in the sample preparation.

(5.) **Orientation examination** of graphene growth was not included in this study. As seen in Figure 4.1, there are some lines that the patches grow along. This can both be the induced flow direction and lines from the fabrication of the copper foil. If these are from the copper foil, polishing of foil may be accurate to try. If these lines are due to the flow of induced gases, further adjustments of gas flow rates may reduce these.

5

Conclusion

Graphene was grown by CVD, and the recipe underwent modifications. Growth from February 21 exhibited many patches but less than the other two growths, and was thus utilized as the reference. As a result, the graphene grown on February 21 transferred to EVA resulted in a mobility of 900-1200 $cm^2/(V{\cdot}s)$. The best quality was received at the center of the copper foil mounted on the quartz tube in the CVD. It was also slightly higher quality of the samples closer to the gas inlet compared to the samples furthest away from the gas inlet. Subsequently, this graphene was directly transferred using REXXAN, resulting in mobility within the same range. It was later transferred using EPO-TEK 730, yielding similar mobility. This confirms that graphene can indeed be transferred using other adhesives capable of withstanding higher temperatures. Moreover, graphene underwent a double transfer, inducing an n-doping effect, thereby resulting in n-doped graphene.

Further examination was conducted on REXXAN and EPO-TEK 730 by directly transferring graphene to a substrate with these adhesives and applying glue on top to observe the doping effect. When applying glue on top of the graphene with many patches (grown on February 21), R_s increased, and n decreased when using both strong and soft etchant. Conversely, when applying glue on top of the bought graphene, which exhibited significantly fewer patches, R_s increased when utilizing a strong etchant but decreased when using a soft etchant or bubbling delamination to remove copper. It was also seen that n decreased more when using softer etchants. However, the absolute value of n became larger when applying glue on top, therefore implying a decrease in mobility when applying glue on top of graphene with few patches.

Of all the graphene grown in this study, February 21 transferred to EPO-TEK 730 resulted in the highest mobility, 1680 $cm^2/(V{\cdot}s)$, when copper was etched with $FeCl_3$. When adding REXXAN glue on top of this sample, mobility increased to 2690 $cm^2/(V{\cdot}s)$.

Bibliography

[1] P.R. Wallace. (1947). The Band Theory of Graphite. Phys. Rev. 71, 622–634.

[2] Boehm, H. P., Setton, R., & Stumpp, E. (1985). Nomenclature and terminology of graphite intercalation compounds. Report by a subgroup of the international committee for characterization and terminology of carbon and graphite on suggestions for rules for the nomenclature and terminology of graphite intercalation compounds. Synthetic Metals, 11(6), 363–371. https://doi.org/10.1016/0379-6779(85)90068-2

[3] Novoselov, K. S., Geim, A. K., Morozov, S. v., Jiang, D., Zhang, Y., Dubonos, S. v., Grigorieva, I. v., & Firsov, A. A. (2004). Electric Field Effect in Atomically Thin Carbon Films. Science, 306(5696), 666–669. https://doi.org/10.1126/science.1102896

[4] Khan, M., Indykiewicz, K., Tam, P., & Yurgens, A. (2022). High Mobility Graphene on EVA/PET. Nanomaterials, 12(3), 331. https://doi.org/10.3390/nano12030331

[5] Choi, S.-S., & Chung, Y. Y. (2020). Simple analytical method for determination of microstructures of poly(ethylene-co-vinyl acetate) using the melting points. Polymer Testing, 90, 106706. https://doi.org/10.1016/j.polymertesting.2020.106706

[6] Levinson, Harry J. (2019). Principles of Lithography (4th Edition). SPIE. Retrieved from https://app.knovel.com/hotlink/toc/id:kpPLE00013/principles-lithography/principles-lithography

[7] Band gap comparison. inductiveload, CC BY-SA 2.5, https://creativecommons.org/licenses/by-sa/2.5, via Wikimedia Commons. Retrieved: June 7, 2024 from https://commons.wikimedia.org/wiki/File:Band_gap_comparison.svg

[8] Wang, Z., Neumaier, D., & Lemme, M. C. (2023). Carbon-Based Field-Effect Transistors (pp. 905–930). https://doi.org/10.1007/978-3-030-79827-7_25

[9] Wilson, M. (2006). Electrons in atomically thin carbon sheets behave like massless particles. Physics Today, 59(1), 21–23.

https://doi.org/10.1063/1.2180163

[10] Neaman, D. A. (2012). Semiconductor Physics and Devices: Basic Principles, Fourth Edition. In McGraw-Hill.

[11] Lee, H., Paeng, K., & Kim, I. S. (2018). A review of doping modulation in graphene. Synthetic Metals, 244, 36–47. https://doi.org/10.1016/j.synthmet.2018.07.001

[12] Hall, E. H. (1879). On a New Action of the Magnet on Electric Currents. American Journal of Mathematics, 2(3), 287. https://doi.org/10.2307/2369245

[13] Hall Effect Measurement Setup for Electrons. CC BY-SA 4.0. https://creativecommons.org/licenses/by-sa/4.0. via Wikimedia Commons. Retrieved: May 30, 2024 from https://commons.wikimedia.org/wiki/File:Hall_Effect_Measurement_Setup_for_Electrons.png

[14] Gausden, J., Siris, R., Stimpel-Lindner, T., McEvoy, N., Duesberg, G. S., & Hallam, T. (2019). Nitrogen as a Suitable Replacement for Argon within Methane-Based Hot-Wall Graphene Chemical Vapor Deposition. Physica Status Solidi (b), 256(12). https://doi.org/10.1002/pssb.201900240

[15] Hugh O. Pierson. (1999). Handbook of Chemical Vapor Deposition (CVD) (Second edition). Noyes Publications / William Andrew Publishing.

[16] Xu, S., Zhang, L., Wang, B., & Ruoff, R. S. (2021). Chemical vapor deposition of graphene on thin-metal films. Cell Reports Physical Science, 2(3), 100372. https://doi.org/10.1016/j.xcrp.2021.100372

[17] Banszerus, L., Schmitz, M., Engels, S., Dauber, J., Oellers, M., Haupt, F., Watanabe, K., Taniguchi, T., Beschoten, B., & Stampfer, C. (2015). Ultrahigh-mobility graphene devices from chemical vapor deposition on reusable copper. Science Advances, 1(6). https://doi.org/10.1126/sciadv.1500222

[18] Yu, Q., Jauregui, L. A., Wu, W., Colby, R., Tian, J., Su, Z., Cao, H., Liu, Z., Pandey, D., Wei, D., Chung, T. F., Peng, P., Guisinger, N. P., Stach, E. A., Bao, J., Pei, S.-S., & Chen, Y. P. (2011). Control and characterization of individual grains and grain boundaries in graphene grown by chemical vapour deposition. Nature Materials, 10(6), 443–449. https://doi.org/10.1038/nmat3010

[19] Yilmaz, M., & Eker, Y. R. (2017). Synthesis of graphene via chemical vapour deposition in copper substrates with different thicknesses. Anadolu university journal of science and technolohy A - Applied Sciences and Engineering, 1–1. https://doi.org/10.18038/aubtda.279709

[20] Kalbac, M., Frank, O., & Kavan, L. (2012). The control of graphene double-layer formation in copper-catalyzed chemical vapor deposition.

Carbon, 50(10), 3682–3687. https://doi.org/10.1016/j.carbon.2012.03.041

[21] Qing, F., Shu, Y., Qing, L., Niu, Y., Guo, H., Zhang, S., Liu, C., Shen, C., Zhang, W., Mao, S. S., Zhu, W., & Li, X. (2018). A general and simple method for evaluating the electrical transport performance of graphene by the van der Pauw–Hall measurement. Science Bulletin, 63(22), 1521–1526. https://doi.org/10.1016/j.scib.2018.10.007

[22] Wu, W., Yu, Q., Peng, P., Liu, Z., Bao, J., & Pei, S.-S. (2012). Control of thickness uniformity and grain size in graphene films for transparent conductive electrodes. Nanotechnology, 23(3), 035603. https://doi.org/10.1088/0957-4484/23/3/035603

[23] Robertson, A. W., & Warner, J. H. (2011). Hexagonal Single Crystal Domains of Few-Layer Graphene on Copper Foils. Nano Letters, 11(3), 1182–1189. https://doi.org/10.1021/nl104142k

[24] Nie, S., Wu, W., Xing, S., Yu, Q., Bao, J., Pei, S., & McCarty, K. F. (2012). Growth from below: bilayer graphene on copper by chemical vapor deposition. New Journal of Physics, 14(9), 093028. https://doi.org/10.1088/1367-2630/14/9/093028

[25] Kim, S., Shin, S., Kim, T., Du, H., Song, M., Lee, C., Kim, K., Cho, S., Seo, D. H., & Seo, S. (2016). Robust graphene wet transfer process through low molecular weight polymethylmethacrylate. Carbon, 98, 352–357. https://doi.org/10.1016/j.carbon.2015.11.027

[26] Leong, W. S., Wang, H., Yeo, J., Martin-Martinez, F. J., Zubair, A., Shen, P.-C., Mao, Y., Palacios, T., Buehler, M. J., Hong, J.-Y., & Kong, J. (2019). Paraffin-enabled graphene transfer. Nature Communications, 10(1), 867. https://doi.org/10.1038/s41467-019-08813-x

[27] Martins, L. G. P., Song, Y., Zeng, T., Dresselhaus, M. S., Kong, J., & Araujo, P. T. (2013). Direct transfer of graphene onto flexible substrates. Proceedings of the National Academy of Sciences, 110(44), 17762–17767. https://doi.org/10.1073/pnas.1306508110

[28] Ren, Y., Zhu, C., Cai, W., Li, H., Hao, Y., Wu, Y., Chen, S., Wu, Q., Piner, R. D., & Ruoff, R. S. (2012). An improved method for transferring graphene grown by chemical vapor deposition. Nano, 07(01), 1150001. https://doi.org/10.1142/S1793292011500019

[29] Hassanpour Amiri, M., Heidler, J., Hasnain, A., Anwar, S., Lu, H., Müllen, K., & Asadi, K. (2020). Doping free transfer of graphene using aqueous ammonia flow. RSC Advances, 10(2), 1127–1131. https://doi.org/10.1039/C9RA06738H

[30] Zhou W, Apkarian R, Wang ZL, Joy D (2006) Fundamentals of scanning electron microscopy (SEM). In: Zhou W., Wang Z.L. (eds). Scanning Microscopy for Nanotechnology. Springer, New York.

https://doi.org/10.1007/978-0-387-39620-0

[31] Krishnasamy, B., Arumugam, H., M, M. I., & Muthukaruppan, A. (2021). Thermal behaviour of benzoxazine blends based on epoxy and cyanate ester. Polymers and Polymer Composites, 29(9_suppl), S1475–S1485. https://doi.org/10.1177/09673911211059714

[32] Gao, L., Ren, W., Xu, H., Jin, L., Wang, Z., Ma, T., Ma, L.-P., Zhang, Z., Fu, Q., Peng, L.-M., Bao, X., & Cheng, H.-M. (2012). Repeated growth and bubbling transfer of graphene with millimetre-size single-crystal grains using platinum. Nature Communications, 3(1), 699. https://doi.org/10.1038/ncomms1702

[33] Pantleon, L., Sousa, T. A. S. L., Jensen, R., Nguyen, D. H., Chau, T. K., Booth, T. J., & Bøggild, P. (2024). Simultaneous dual-configuration van der Pauw measurements of gated graphene devices. Measurement, 225, 113954. https://doi.org/10.1016/j.measurement.2023.113954

[34] Yurgens, A. (2024). CVD (Chemical Vapor Deposition) of graphene Lab PM.

A

Equipment

A.1 CVD equipment

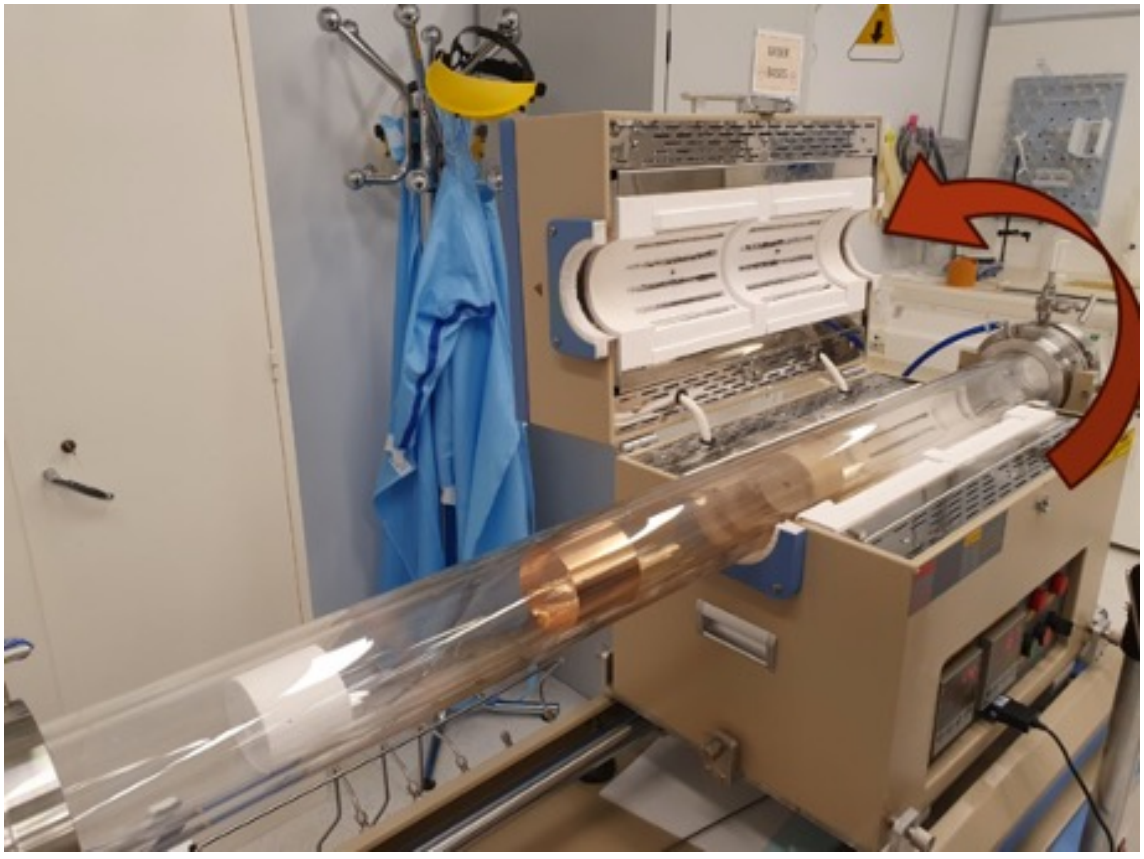

Figure A.1: Copper foil mounted in MTI OTF-1200X. Here the chamber is open, and about to be slid into position, center of the copper foil. Image adopted from [34].

A.2 Transfer equipment

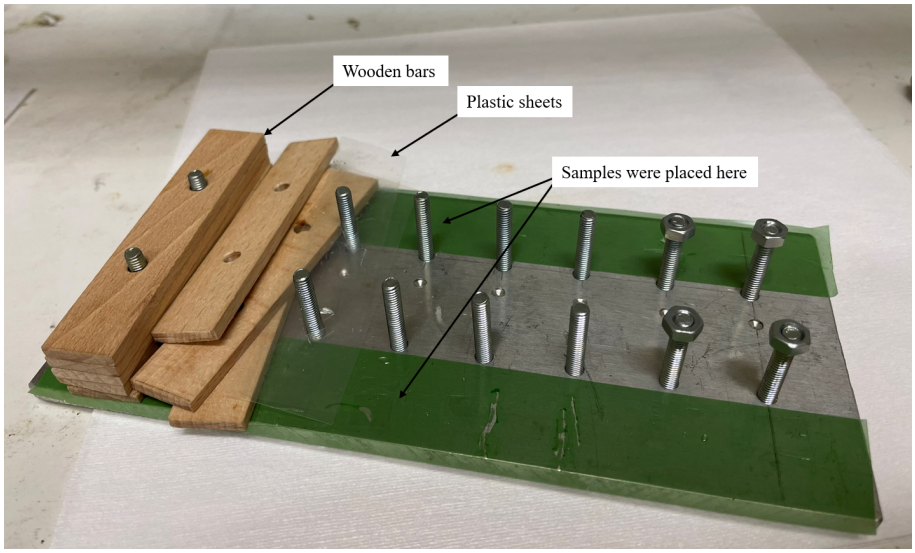

Figure A.2: Equipment that applies pressure during curing time. The samples were placed on the green; wooden bars were applied on top, and thin plastic sheets were used to ensure the adhesive did not stick to the wood or green surface. A weight was placed on top of these.

(a) **(b)**

Figure A.3: **(a)** Small chamber with nitrogen flow. Samples were placed in this, and a lid was applied on top. **(b)** Rubber roller was used on the lid of the small chamber in the double transfer process.

A.3 Measuring equipment

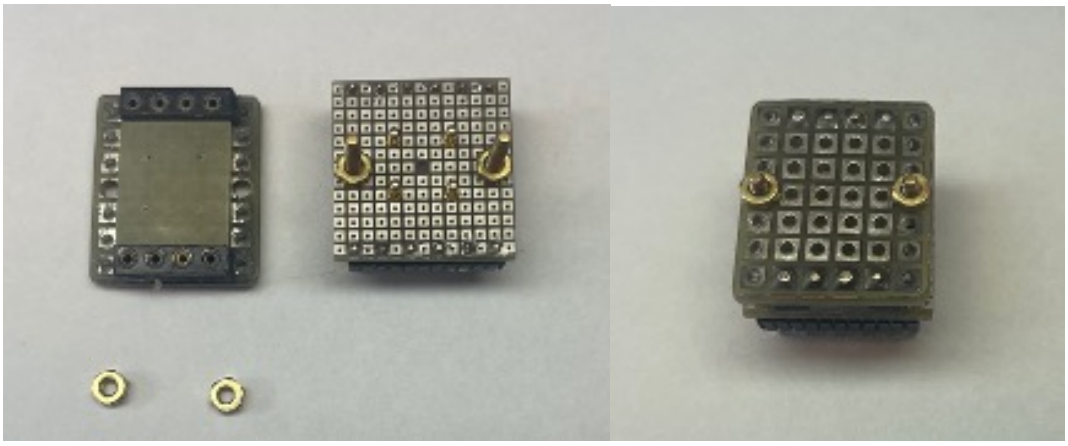

(a) **(b)**

Figure A.4: Rigg with four probes; **(a)** disassembled and **(b)** assembled

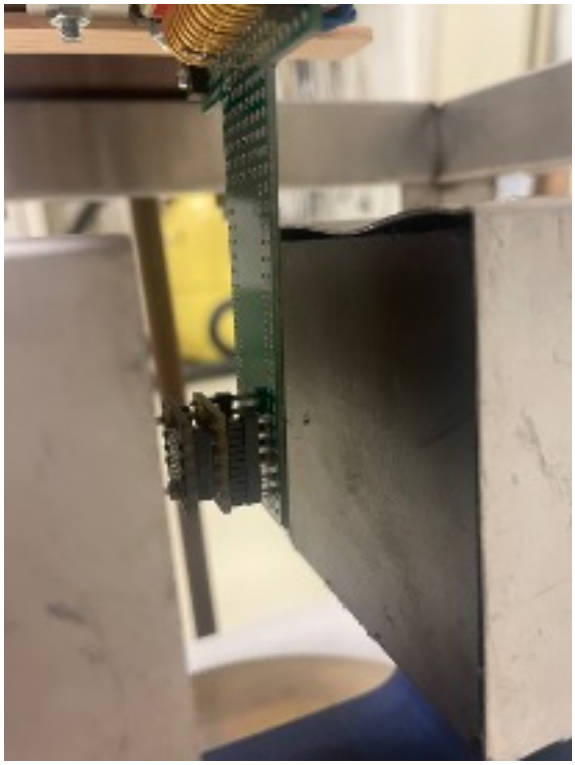

Figure A.5: Rigg with four probes mounted in a magnetic field provided by a U-shaped magnet.

B

Annealing

B.1 Graphene grown on February 15 and February 21, annealed in 60°C

Table B.1: Graphene grown on February 15 transferred to EVA/PET foil, copper etched in HNO_3, samples washed in ethanol for 5 minutes and annealed 60°C 3 days.

Position	1	2	3	4	5	6
R_s [Ω/□]	11600	10830	9630	15600	27040	11100
μ [cm^2/(V·s)]	487	577	695	372	282	337
R_H [Ω/□]	89.2	98.1	105.0	91.0	119.0	589
n [10^{12} cm^{-2}]	1.1	1.0	0.9	1.1	0.8	0.2

Table B.2: Graphene grown on February 21 transferred to EVA/PET foil, copper etched in HNO_3, samples washed in ethanol for 5 minutes and annealed 60°C 4 days.

Position	1	2	3	4	5	6
R_s [Ω/□]	3070	3820	3240	3770	4490	3820
μ [cm^2/(V·s)]	745	834	1020	952	725	703
R_H [Ω/□]	35.9	50.1	52.0	56.4	51.1	42.2
n [10^{12} cm^{-2}]	2.7	2.0	1.9	1.7	1.9	2.3

C

Additional direct- & double transfer

C.1 Direct- & double transfer with Araldite and EPO-TEK 323

Table C.1: Direct- & double transfer with graphene grown on February 21 with Araldite and EPO-TEK 323. Parafilm was used as a preliminary substrate during double transfer. Copper was etched in HNO_3.

		Araldite	EPO-TEK 323
Direct	R_s [Ω/□]	2760	469
	μ [cm^2/(V·s)]	385	645
	R_H [Ω/□]	16.7	4.8
	n [10^{12} cm^{-2}]	5.9	20.6
Double	R_s [Ω/□]	1810	1560
	μ [cm^2/(V·s)]	-540	-1650
	R_H [Ω/□]	-15.4	-40.5
	n [10^{12} cm^{-2}]	-6.4	-2.4

D

Test methods

D.1 Direct transfer comparing samples without- and with shaped samples

Table D.1: Direct transfer graphene growth February 21, with EPO-TEK 730 (B). Copper was etched in HNO_3. Data was collected before and after shaping samples as illustrated in Figure 3.4(a) and Figure 3.4(b). EPO-TEK 730 and REXXAN (A) was applied as top glue illustrated in Figure 3.4(c).

		B/-	B/-
Fig. 3.4(a)	R_s [$\Omega/\square$]	508	994
	μ [$cm^2/(V{\cdot}s)$]	385	158
	R_H [$\Omega/\square$]	3.0	2.5
	n [10^{12} cm^{-2}]	31.9	39.8
Fig. 3.4(b)	R_s [$\Omega/\square$]	531	1360
	μ [$cm^2/(V{\cdot}s)$]	420	209
	R_H [$\Omega/\square$]	3.5	4.5
	n[10^{12} cm^{-2}]	28.0	22.0
		B/B	B/A
Fig. 3.4(c)	R_s [$\Omega/\square$]	2340	5770
	μ [$cm^2/(V{\cdot}s)$]	-277	339
	R_H [$\Omega/\square$]	-10.2	30.7
	n [10^{12} cm^{-2}]	-9.6	3.2
	Δ R_s	+340 %	+324 %
	Δ n	-134 %	-85 %

D.2 Impact of applying silver glue to increase contact with probes

Table D.2: Three samples of graphene grown on February 21, direct transferred on REXXAN and Araldite. Copper was etched in HNO_3. Tested both without and with silver glue at the contact points for the probes.

		#1 REXXAN	#2 REXXAN	#3 Araldite
Without	R_s [$\Omega/\square$]	2360	1950	2760
	μ [$cm^2/(V{\cdot}s)$]	1160	1390	385
	R_H [$\Omega/\square$]	42.8	42.5	16.7
	n [10^{12} cm^{-2}]	2.3	2.3	5.9
With	R_s [$\Omega/\square$]	4650	2870	2950
	μ [$cm^2/(V{\cdot}s)$]	326	643	309
	R_H [$\Omega/\square$]	23.8	29.0	14.3
	n [10^{12} cm^{-2}]	4.1	3.4	6.8

E

Additional samples with top gluing

E.1 Direct transfer on EVA, adhesives applied on top

Table E.1: Four samples of graphene grown on February 21, directly transferred on EVA, copper was etched in HNO_3, and samples were washed in ethanol. The lower part of the table represents when top glue was applied.

		EVA/-	EVA/-	EVA/-	EVA/-
Fig. 3.4b	R_s [$\Omega/\square$]	2180	1980	2260	1950
	μ [$cm^2/(V{\cdot}s)$]	802	904	830	957
	R_H [$\Omega/\square$]	27.4	28.2	29.5	29.3
	n [10^{12} cm^{-2}]	3.6	3.5	3.3	3.4
Top glue		EVA/REXXAN	EVA/Araldite	EVA/Contact glue	EVA/EPO-TEK 730
Fig. 3.4c	R_s [$\Omega/\square$]	1670	804	2220	902
	μ [$cm^2/(V{\cdot}s)$]	-876	-782	-608	-1150
	R_H [$\Omega/\square$]	-22.9	-9.9	-21.2	-16.2
	n [10^{12} cm^{-2}]	-4.3	-9.9	-4.6	-6.0
ΔR_s		-23 %	-59 %	-2 %	-56 %
Δn		-219 %	-383 %	-239 %	-276 %

E.2 Direct transfer on REXXAN and EPO-TEK 730, Araldite and contact glue applied on top

Table E.2: Results from top gluing on direct transferred graphene grown February 21 on REXXAN (A) and EPO-TEK 730 (B). Araldite and contact glue were used as top glues. Copper was etched in HNO_3.

		A/-	A/-	B/-	B/-
Fig. 3.4b	R_s [Ω/□]	312	400	1570	1490
	μ [cm^2/(V·s)]	1420	1130	334	281
	R_H [Ω/□]	6.9	7.1	8.2	6.6
	n [10^{12} cm^{-2}]	14.1	13.9	11.9	14.9
		A/Araldite	A/Contact glue	B/Araldite	B/Contact glue
Fig. 3.4c	R_s [Ω/□]	332	3540	1940	2010
	μ [cm^2/(V·s)]	-1700	847	-443	367
	R_H [Ω/□]	-8.9	47.1	-13.5	11.6
	n [10^{12} cm^{-2}]	-11.1	2.1	-7.3	8.5
	Δ R_s	+6 %	+785 %	+24 %	+35 %
	Δ n	-179 %	-85 %	-161 %	-44 %

E.3 Direct transfer of bought graphene with REXXAN, REXXAN applied on top

Table E.3: Two samples of bought graphene directly transferred with REXXAN (A). Copper was etched with HNO_3. REXXAN was here also applied as top glue.

		A/-	A/-
Fig. 3.4(b)	R_s [Ω/□]	1220	920
	μ [cm^2/(V·s)]	1340	2090
	R_H [Ω/□]	25.7	30.1
	n [10^{12} cm^{-2}]	3.8	3.3
		A/A	A/A
Fig. 3.4(c)	R_s [Ω/□]	8560	5370
	μ [cm^2/(V·s)]	-1130	-2020
	R_H [Ω/□]	-151.7	-169.9
	n [10^{12} cm^{-2}]	-0.6	-0.6
	Δ R_s	+602 %	+484 %
	Δ n	-116 %	-118 %

E.4 Direct transfer on REXXAN and EPO-TEK 730, REXXAN and EPO-TEK 730 applied on top

Table E.4: Results from applying glues on top of direct transferred graphene grown on February 21. REXXAN (A) and EPO-TEK 730 (B). Copper was etched in HNO_3.

	A/-	B/-
R_s [$\Omega/\square$]	928	511
μ [$cm^2/(V{\cdot}s)$]	1070	841
R_H [$\Omega/\square$]	15.6	6.7
n [10^{12} cm^{-2}]	6.3	14.5
	A/A	B/A
R_s [$\Omega/\square$]	769	2400
μ [$cm^2/(V{\cdot}s)$]	-1220	646
R_H [$\Omega/\square$]	-14.7	24.3
n [10^{12} cm^{-2}]	-6.7	4.0
Δ R_s	-17 %	+369 %
Δ n	-206 %	-72 %

DEPARTMENT OF SOME SUBJECT OR TECHNOLOGY
CHALMERS UNIVERSITY OF TECHNOLOGY
Gothenburg, Sweden
www.chalmers.se

CHALMERS
UNIVERSITY OF TECHNOLOGY